Physics of neutron-rich nuclei

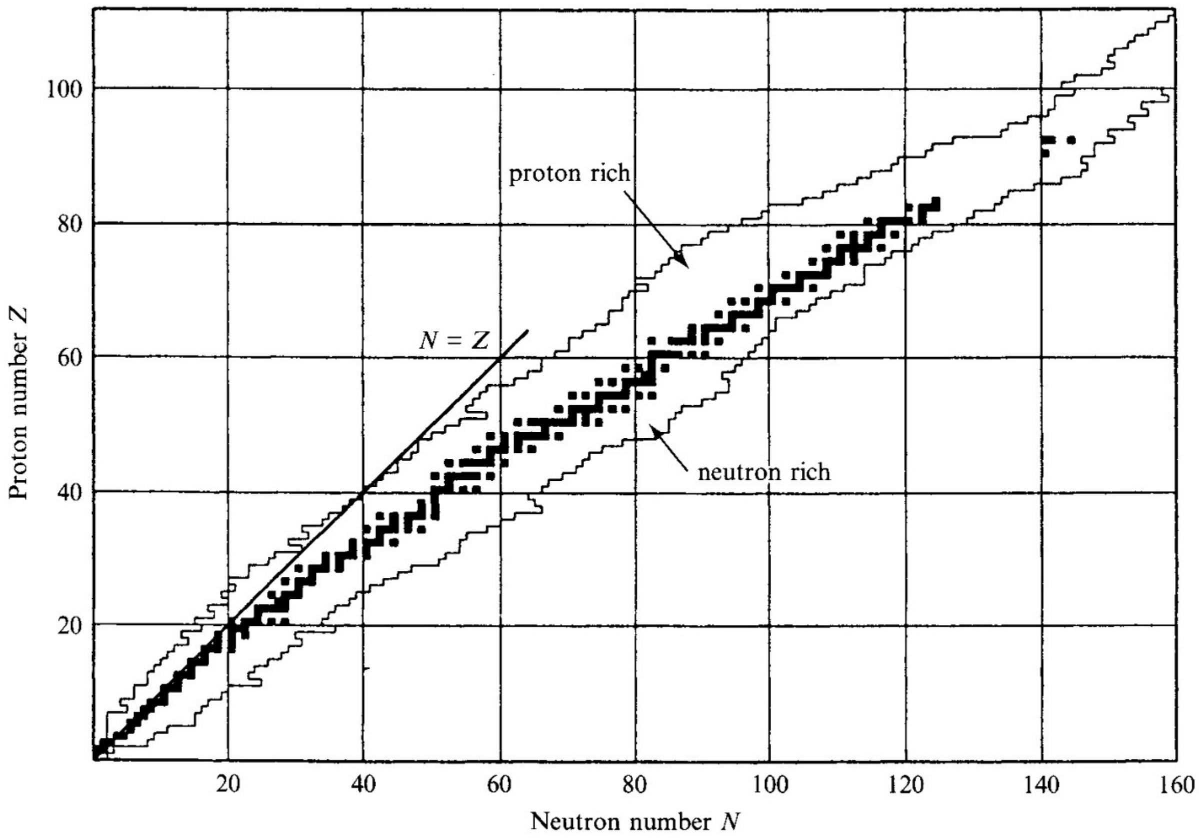

Nuclear Physics: developed for stable nuclei (until the mid 1980’s)

saturation, radii, binding energy,
magic numbers and independent particle….

Physics of neutron-rich nuclei

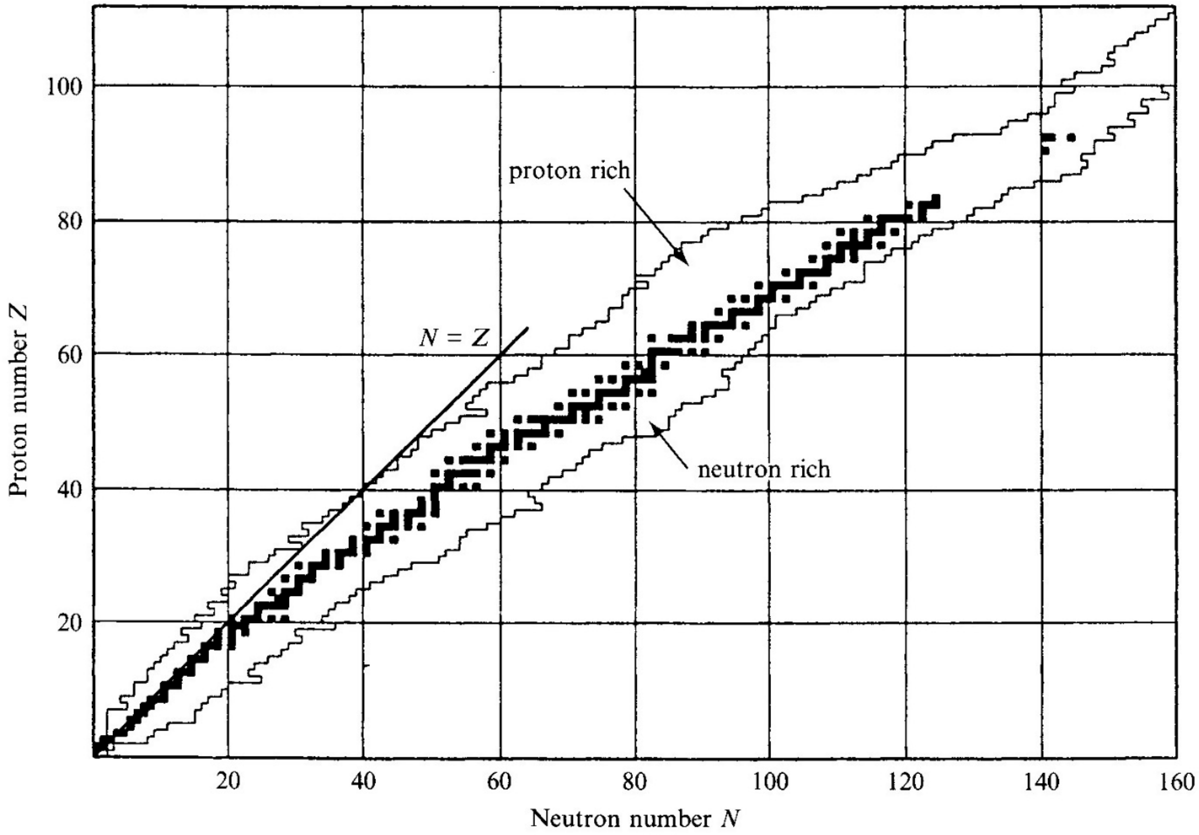

Nuclear Physics: developed for stable nuclei (until the mid 1980's)

- how many neutrons can be put into a nucleus when the number of proton is fixed?
- what are the properties of nuclei far from the stability line?

Physics of neutron-rich nuclei

characteristic features of nuclei close to the neutron-drip line?

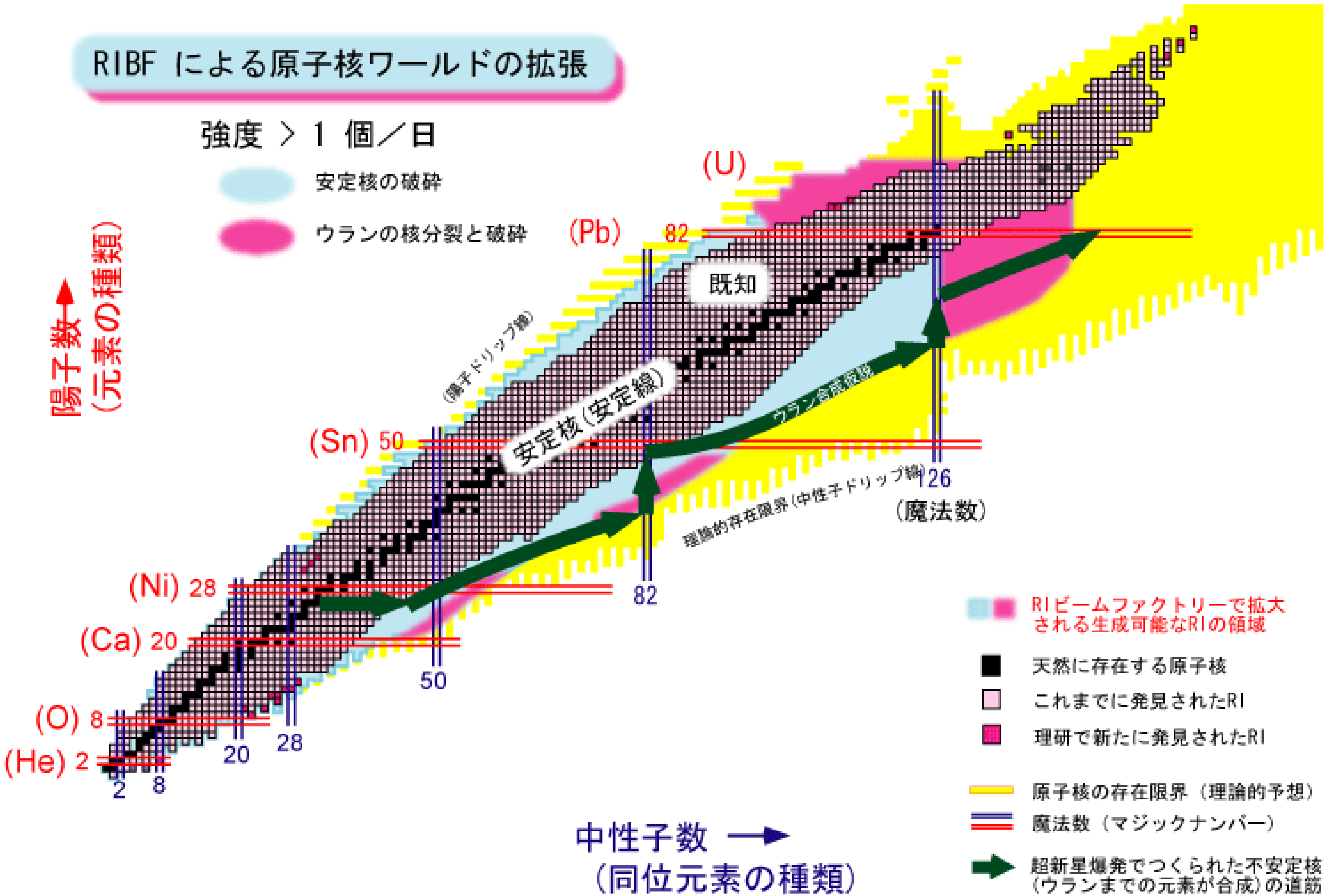

Physics of unstable nuclei

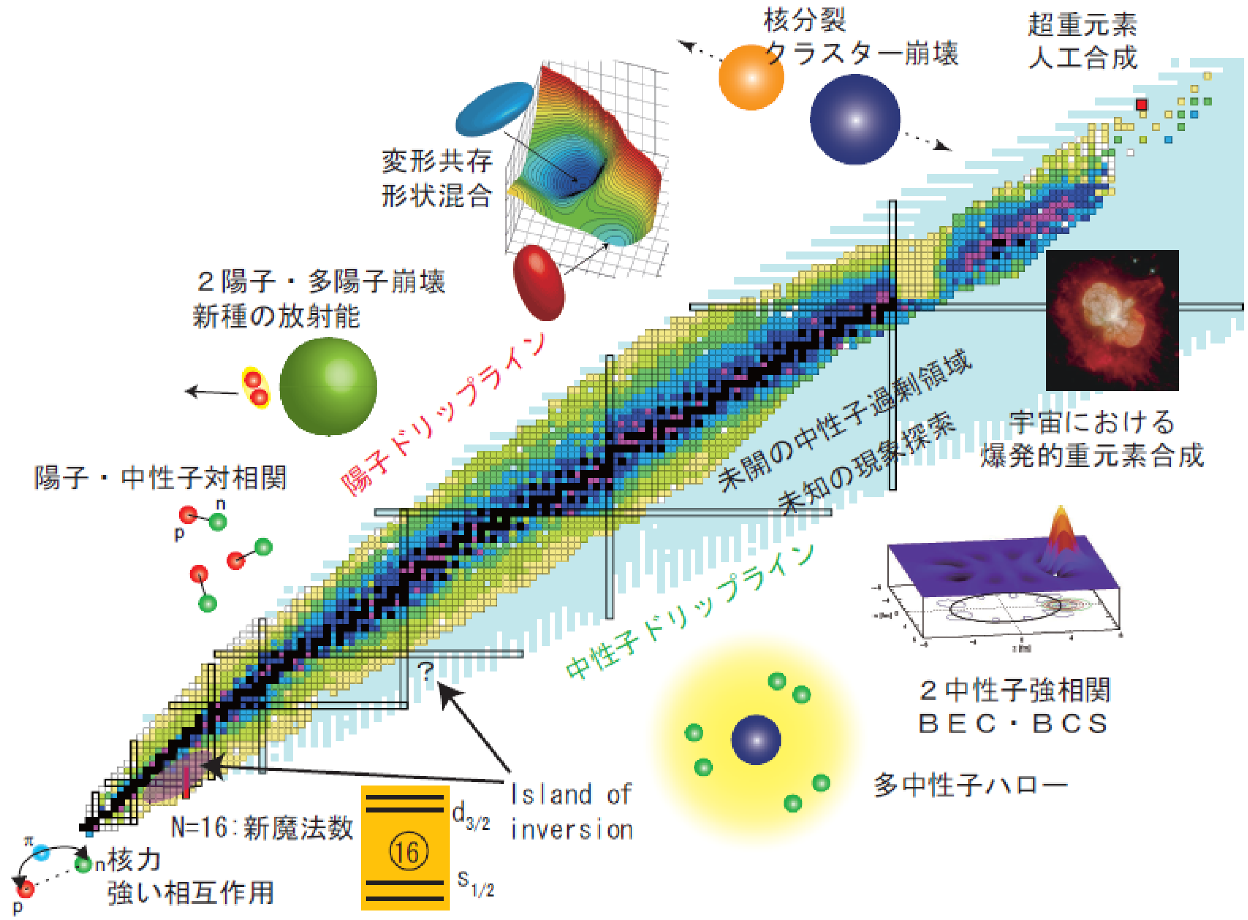

- ✓ Unveil new properties of atomic nuclei by controlling the proton and neutron numbers
- ✓ Explore the new phases and dynamics of nuclear matter at several proton and neutron densities

New generation RI beam facility: RIKEN RIBF
(Radioactive Isotope Beam Factory)

a facility to create unstable nuclei with the world largest intensity

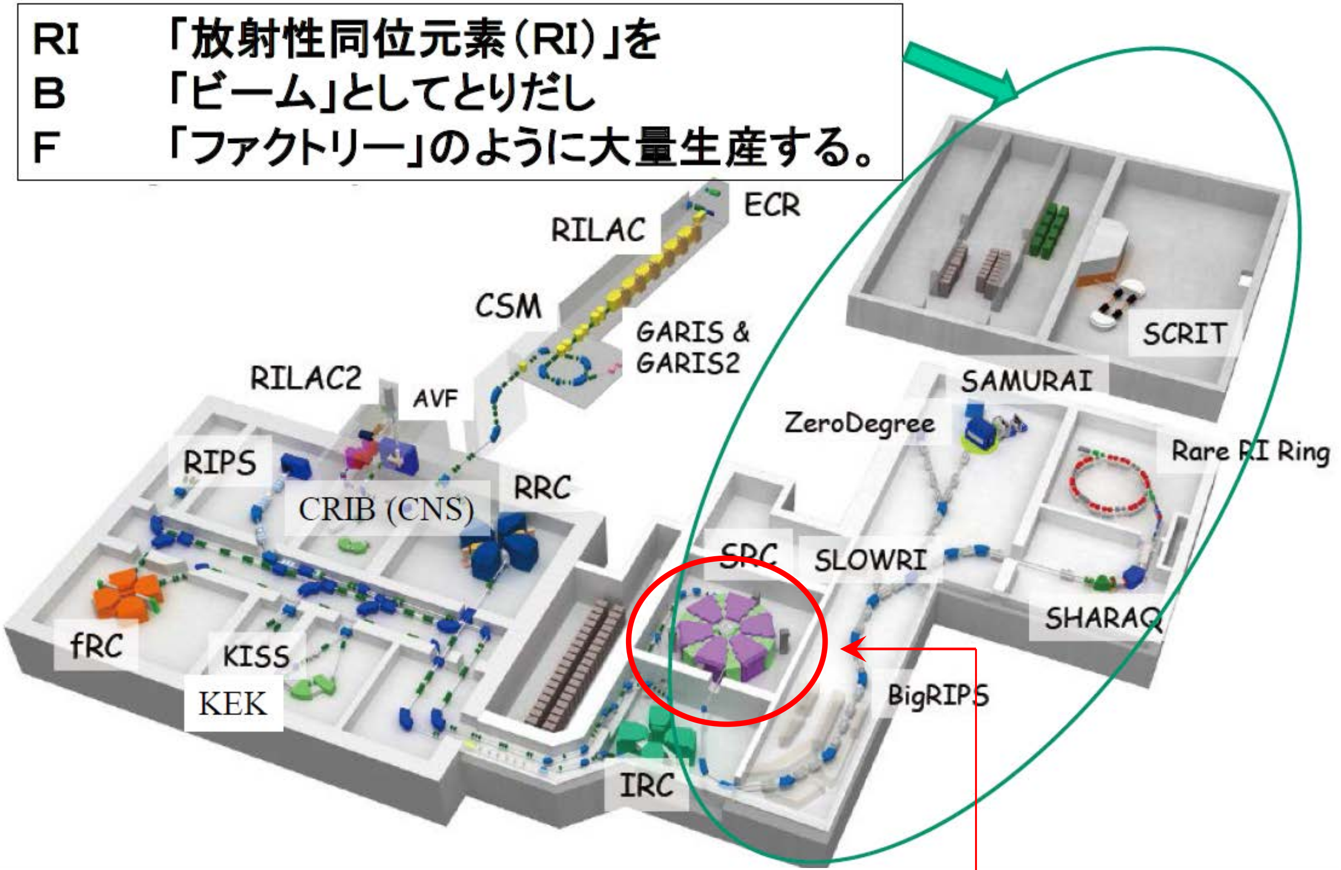

- physics of unstable nuclei
- the origin of elements
- superheavy nuclei

A start of a research on unstable nuclei: interaction cross sections (1985)

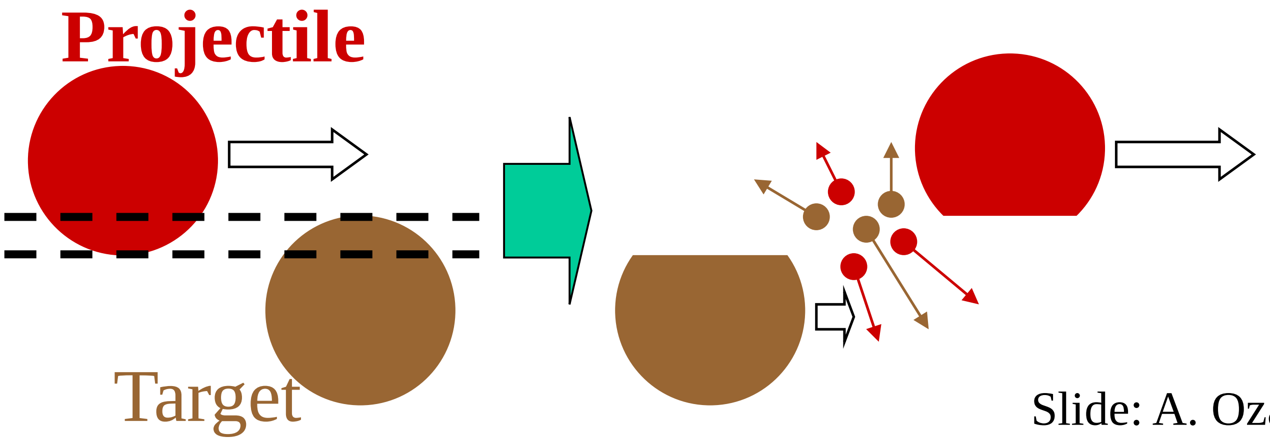

Slide: A. Ozawa

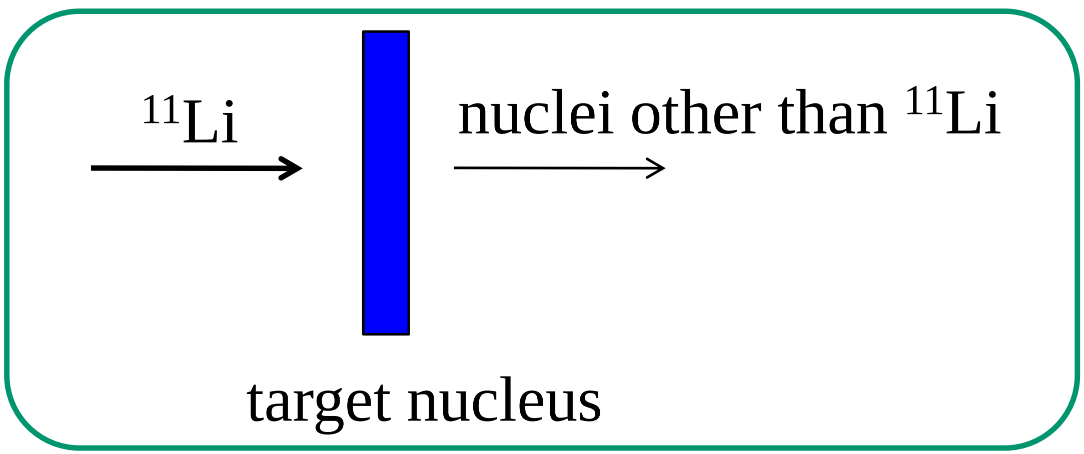

if reaction takes place when overlap:

$$\sigma_I \sim \pi[R_I(P) + R_I(T)]^2$$

$\longrightarrow$ R_I(P)

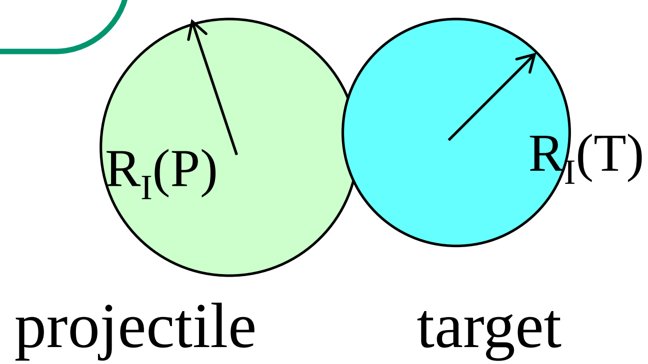

A start of a research on unstable nuclei: interaction cross sections (1985)

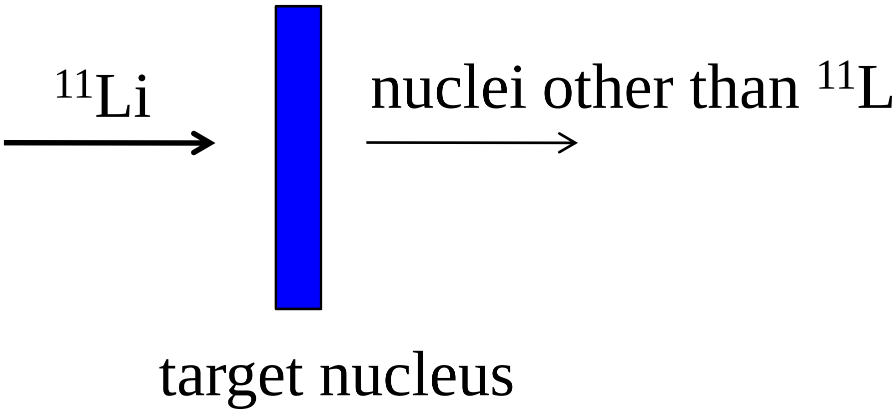

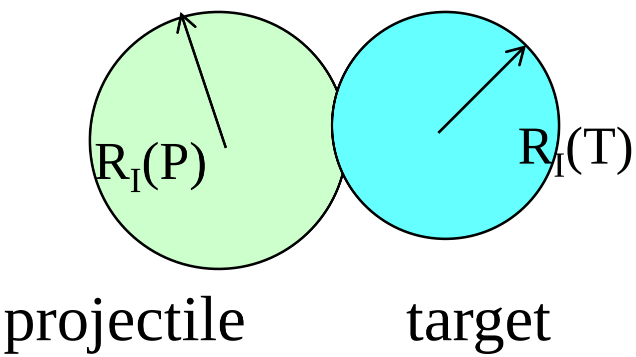

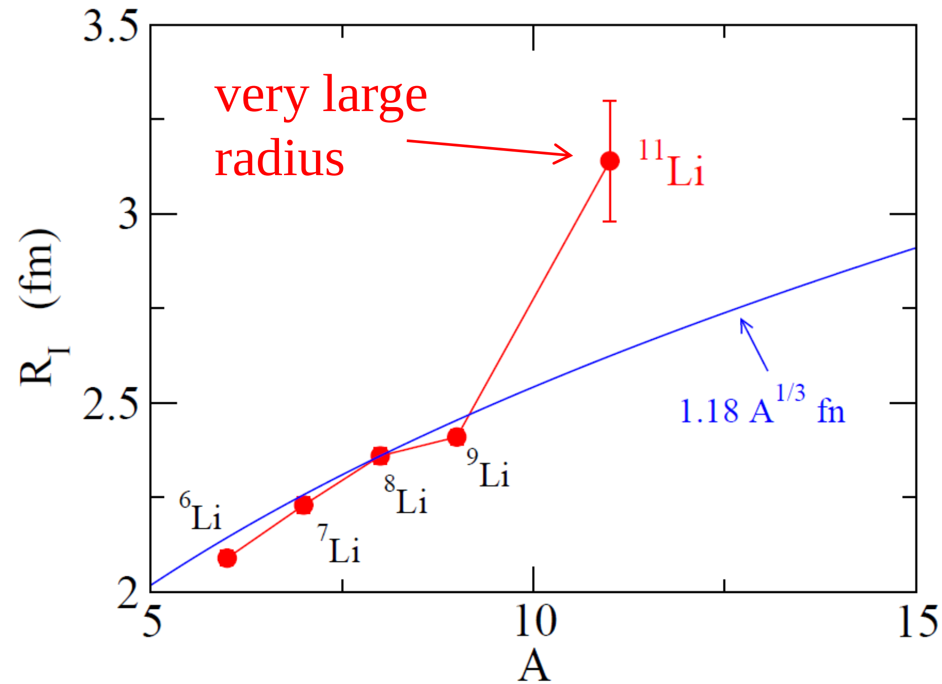

I. Tanihata et al., PRL55('85)2676

if reaction takes place when overlap:

$$\sigma_I \sim \pi[R_I(P) + R_I(T)]^2$$

$$\longrightarrow \quad R_I(P)$$

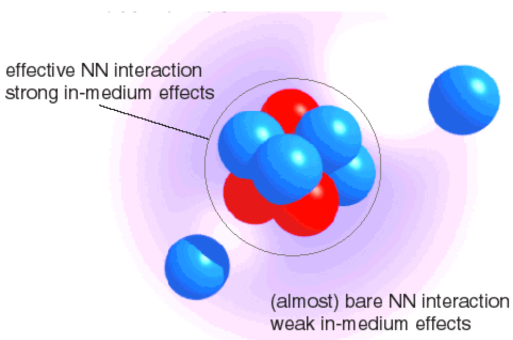

One neutron halo nuclei

A typical example: ${}^{11}_{4}Be_7$

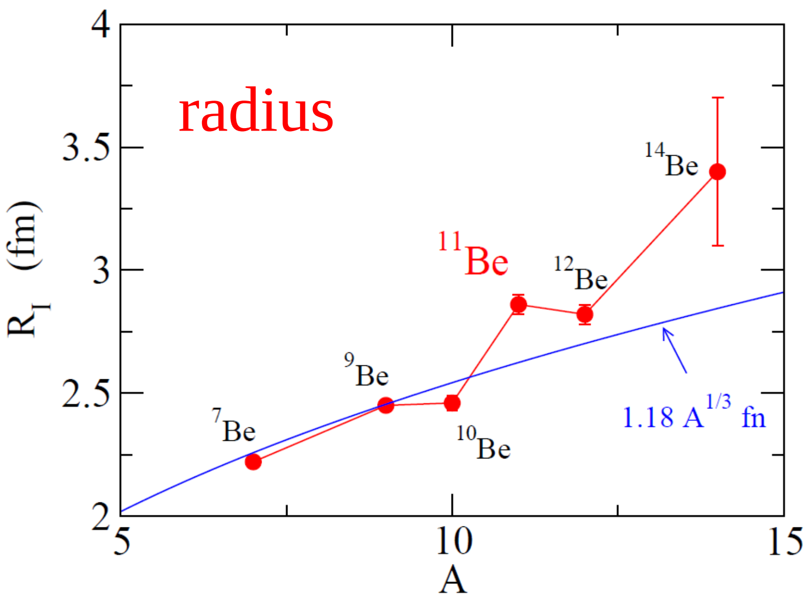

I. Tanihata et al.,
PRL55('85)2676; PLB206('88)592

One neutron separation energy

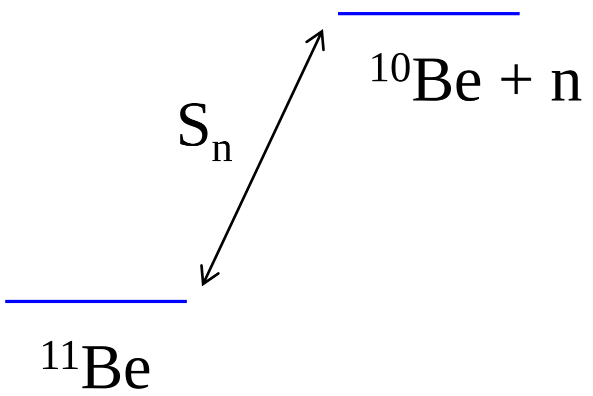

S_n = 504 +/- 6 keV

very small

cf. S_n = 4.95 MeV
for ^{13}C

One neutron halo nuclei

A typical example: $^{11}_{4}\mathrm{Be}_{7}$

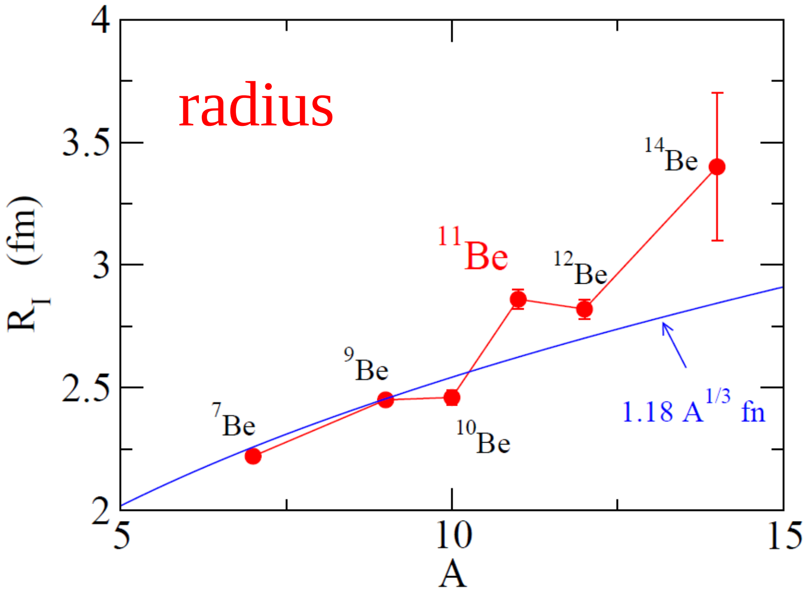

One neutron separation energy

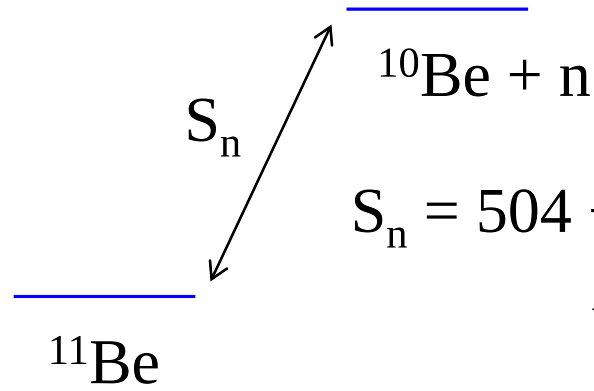

S_n = 504 +/- 6 keV

very small

Interpretation : a weakly bound neutron surrounding ^{10}Be

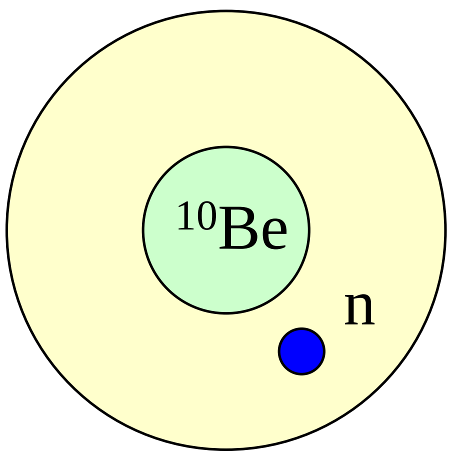

$$\psi(r) \sim \exp(-\kappa r) \qquad \kappa = \sqrt{2m|\epsilon|/\hbar^2}$$

weakly bound system

⇓

large spatial extension of density (halo structure)

Interpretation : a weakly bound neutron surrounding ^{10}Be

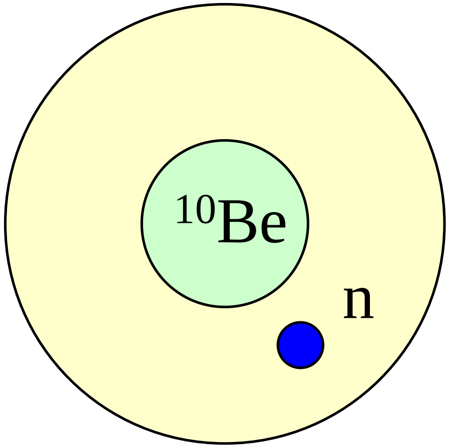

$$\psi(r) \sim \exp(-\kappa r) \qquad \kappa = \sqrt{2m|\epsilon|/\hbar^2}$$

weakly bound system

↓

large spatial extension of density (halo structure)

Density distribution which explains
the experimental reaction cross section

lunar halo
(a thin ring around moon)

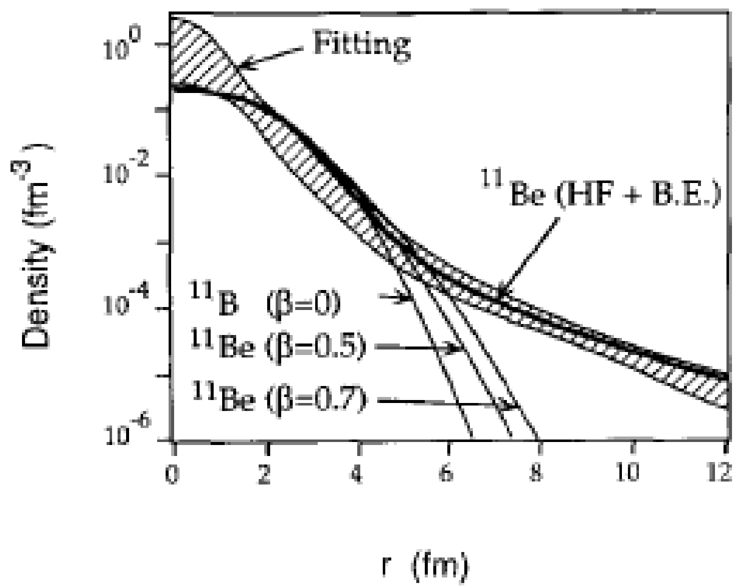

M. Fukuda et al., PLB268('91)339

Momentum distribution

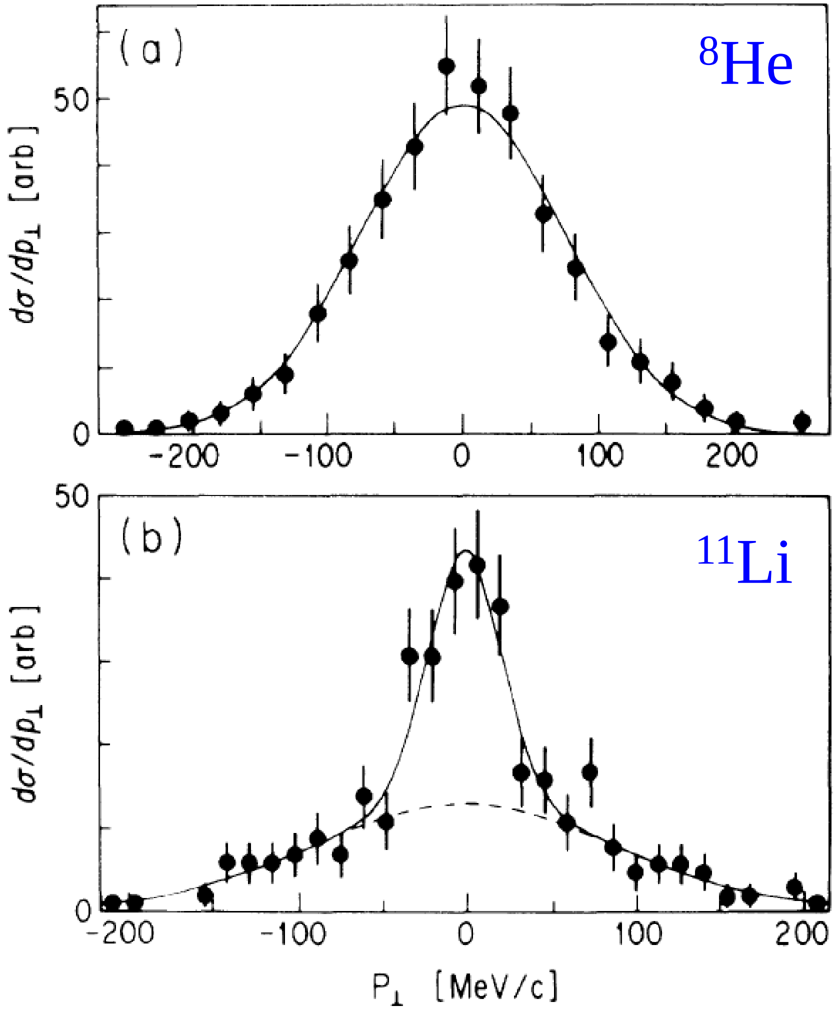

FIG. 1. Transverse-momentum distributions of (a) ^{6}He fragments from reaction ^{8}He+C and (b) ^{9}Li fragments from reaction ^{11}Li+C. The solid lines are fitted Gaussian distributions. The dotted line is a contribution of the wide component in the ^{9}Li distribution.

S_{2n} ~ 2.1 MeV

S_{2n} ~ 300 keV

a narrow mom. distribution when weakly bound and thus a large spatial extension

↔ neutron halo

T. Kobayashi et al., PRL60 ('88) 2599

Properties of single-particle motion: bound state

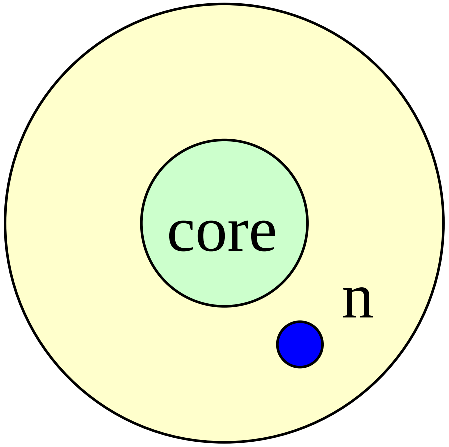

assume a 2body system with a core nucleus and a valence neutron

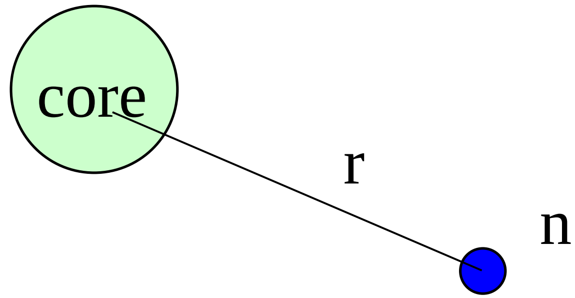

consider a spherical potential $V(r)$ as a function of r

cf. mean-field potential:

$$V(\boldsymbol{r}) \sim \int v(\boldsymbol{r}, \boldsymbol{r}')\rho(\boldsymbol{r}')d\boldsymbol{r}'$$

Hamiltonian for the relative motion

$$H = -\frac{\hbar^2}{2\mu}\nabla^2 + V(r)$$

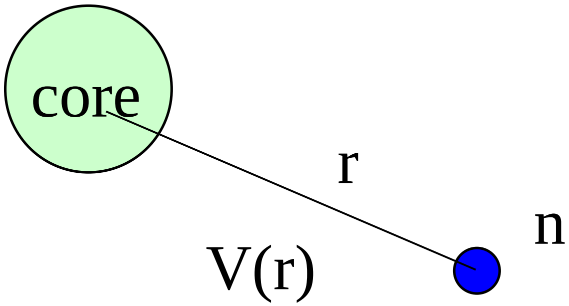

Hamiltonian for the relative motion

$$H = -\frac{\hbar^2}{2\mu}\nabla^2 + V(r)$$

For simplicity, let us ignore the spin-orbit interaction
(the essence remains the same even if no spin-orbit interaction)

$$\Psi_{lm}(\boldsymbol{r}) = \frac{u_l(r)}{r} Y_{lm}(\hat{\boldsymbol{r}})$$

$$\left[-\frac{\hbar^2}{2\mu}\frac{d^2}{dr^2} + \frac{l(l+1)\hbar^2}{2\mu r^2} + V(r) - \epsilon_l\right] u_l(r) = 0$$

Boundary condition for bound states

$$u_l(r) \sim r^{l+1} \quad (r \sim 0)$$
$$\to e^{-\kappa r} \quad (r \to \infty)$$

* For a more consistent treatment, a modified spherical Bessel function has to be used

Angular momentum and halo phenomenon

$$\left[-\frac{\hbar^2}{2\mu}\frac{d^2}{dr^2}+\frac{l(l+1)\hbar^2}{2\mu r^2}+V(r)-\epsilon_l\right]u_l(r)=0$$

Centrifugal potential

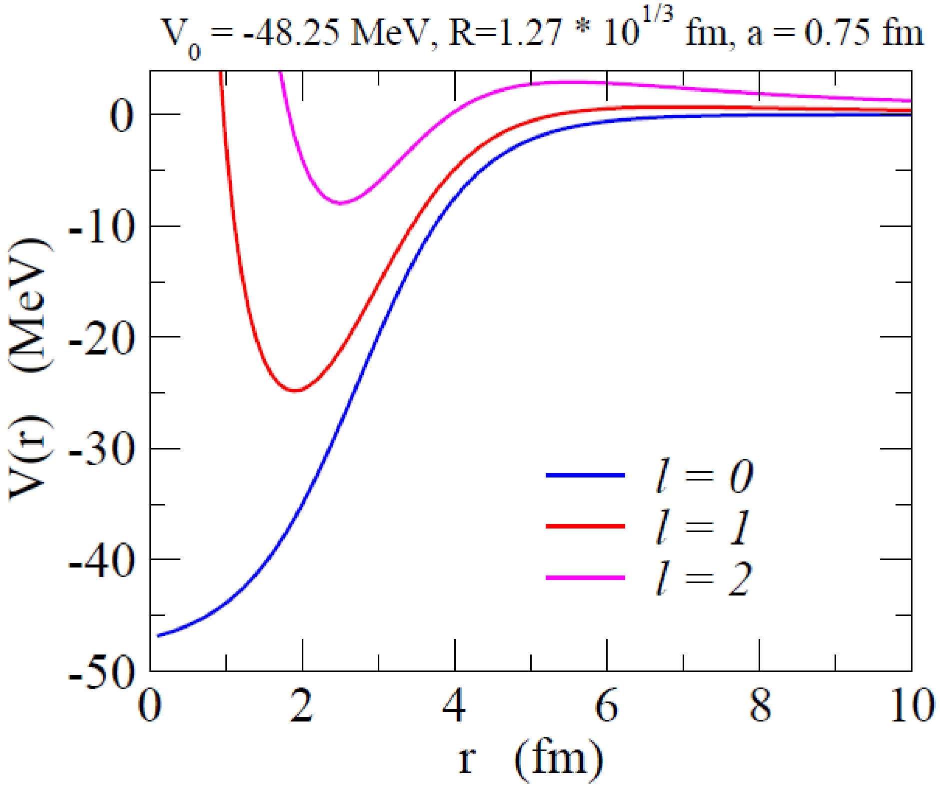

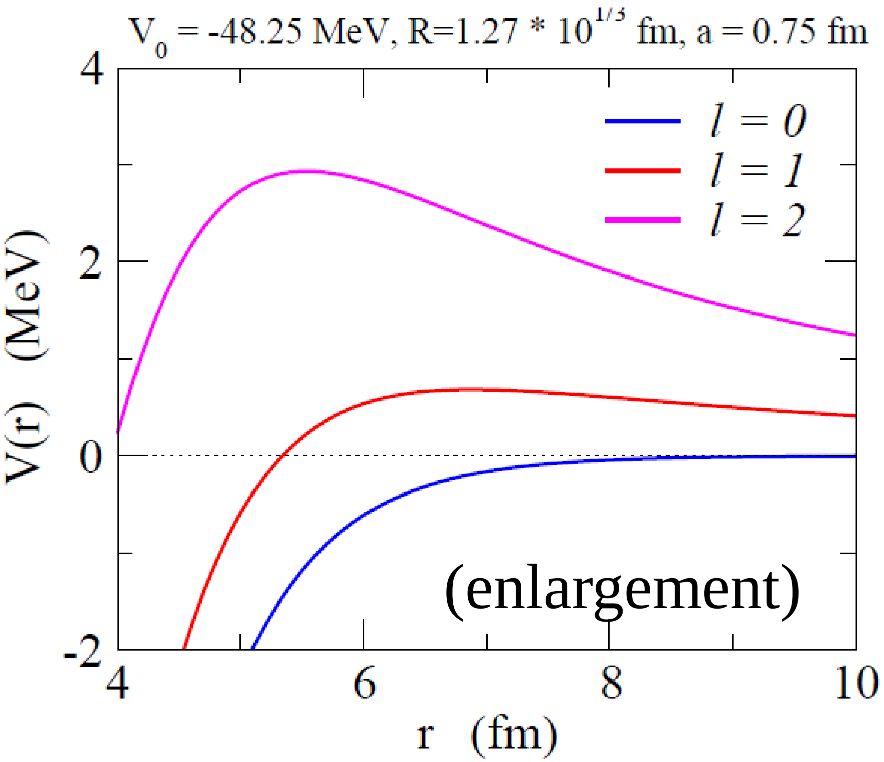

The height of centrifugal barrier: 0 MeV (l = 0), 0.69 MeV (l = 1), 2.94 MeV (l = 2)

Wave function Change V_0 for each l so that ε = -0.5 MeV

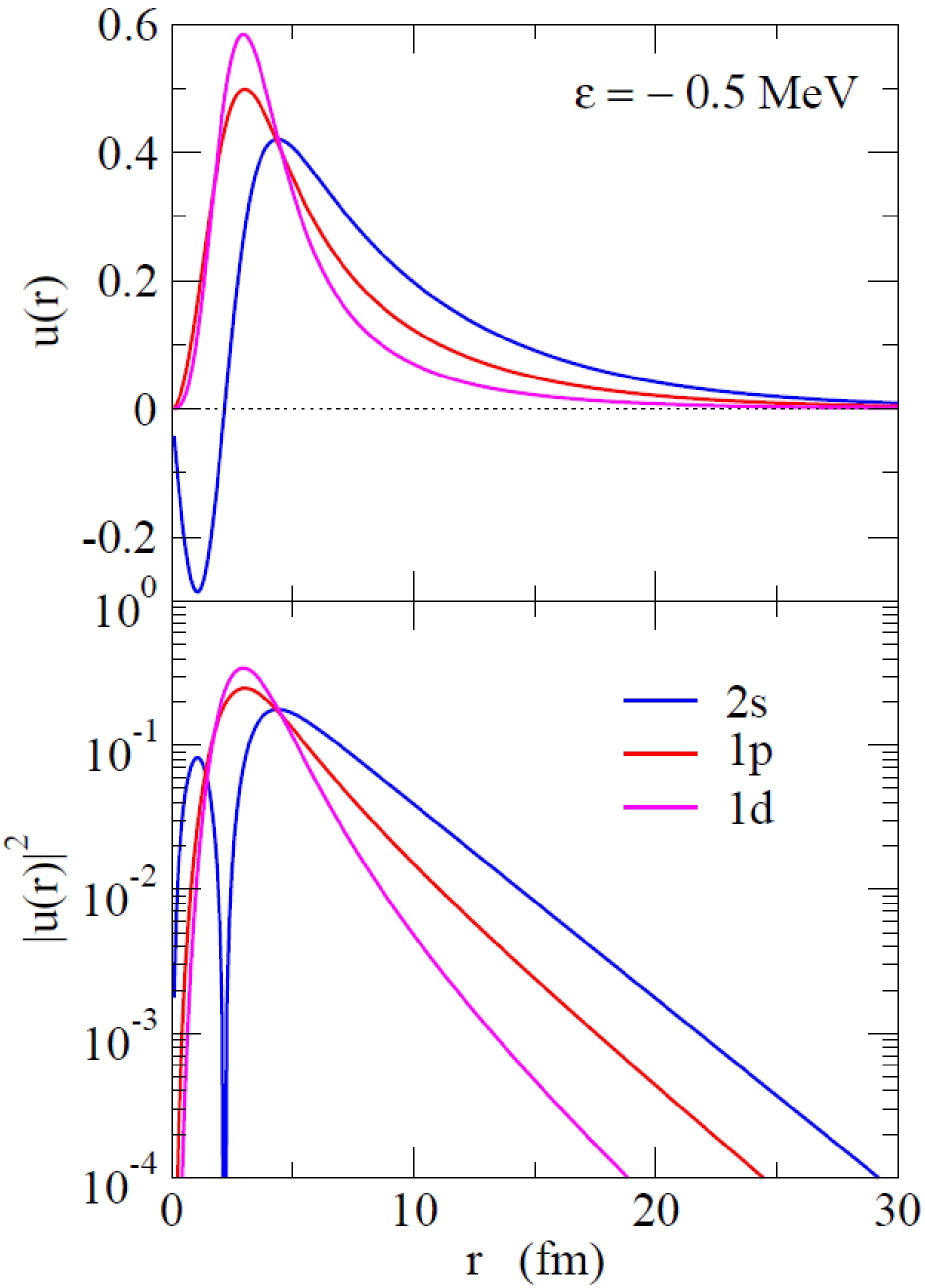

l = 0 : a long tail
l = 2 : localization
l = 1 : intermediate

root-mean-square radius

$$\sqrt{\langle r^2 \rangle} = \sqrt{\int_0^\infty dr\, r^2 u_l(r)^2}$$

7.17 fm (l = 0)
5.17 fm (l = 1)
4.15 fm (l = 2)

Wave functions

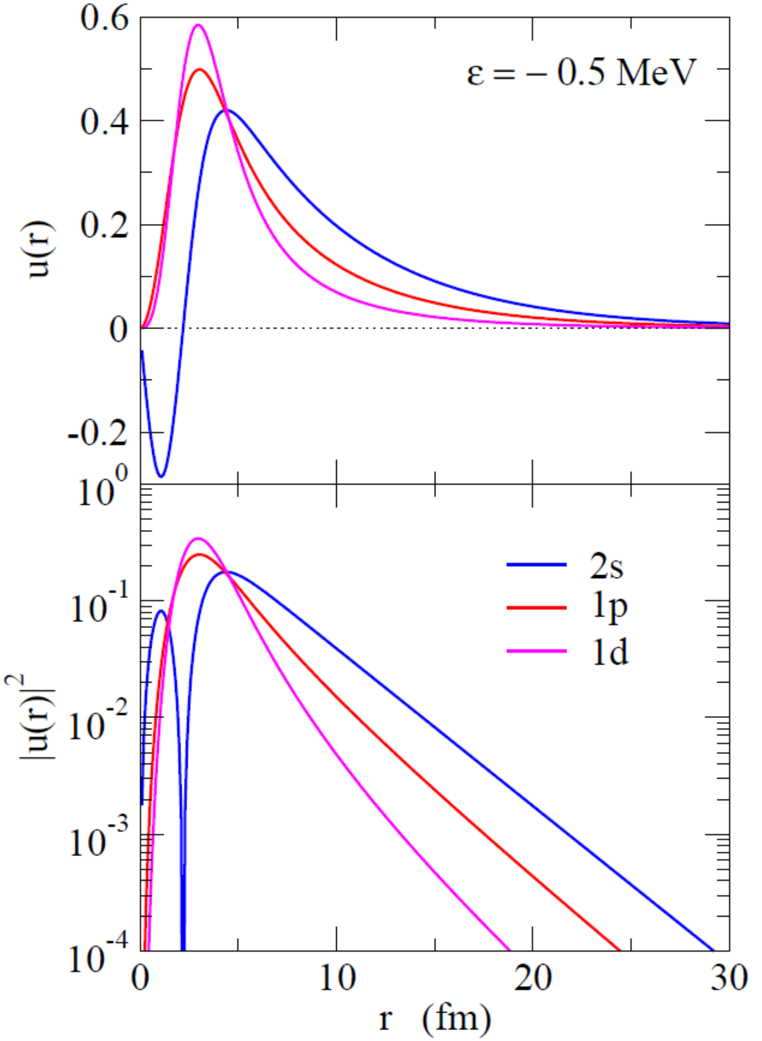

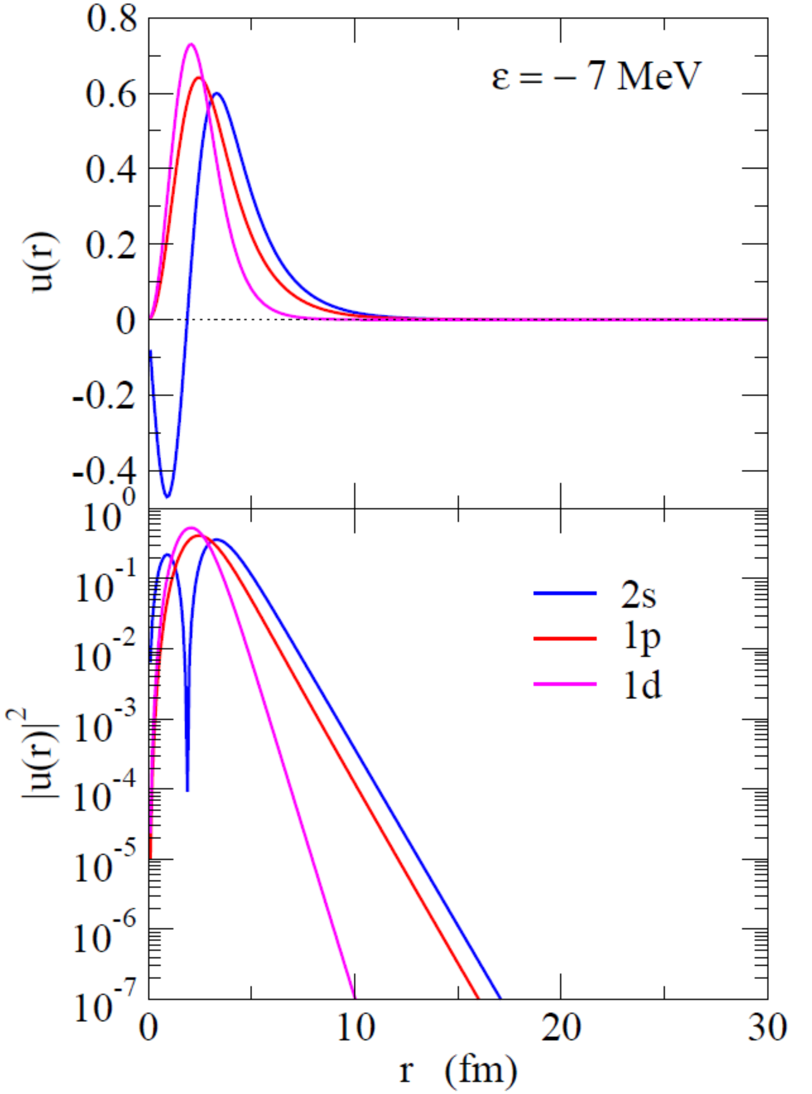

$$\langle r^2 \rangle \propto \begin{cases} 1/|\epsilon_0| & (l=0) \\ 1/\sqrt{|\epsilon_1|} & (l=1) \\ const. & (l=2) \end{cases}$$

⇩

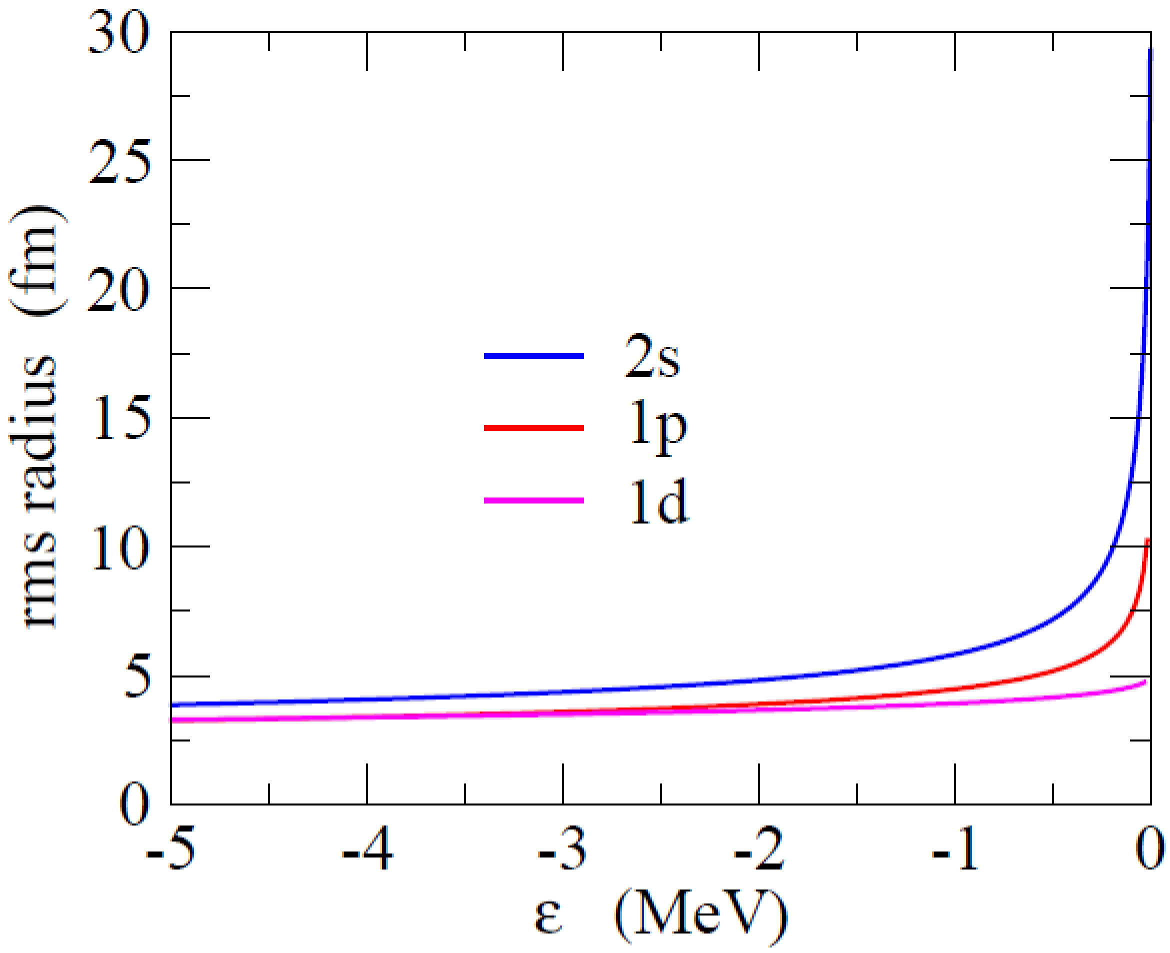

Radius: diverges for *l*=0 and 1 in the zero energy limit

⇩

Halo (a very large radius) happens only for *l*= 0 or 1

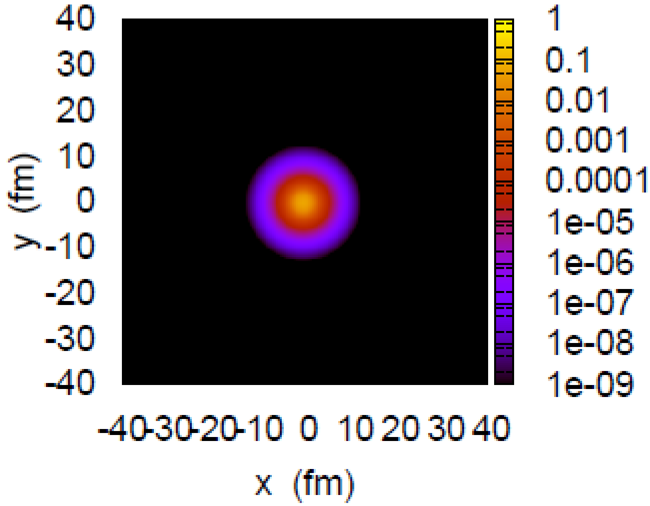

e = -8.07 MeV

V_0 = 24 MeV
R = 2.496 fm

weakly
bound

a l=0 bound state
in a square well pot.

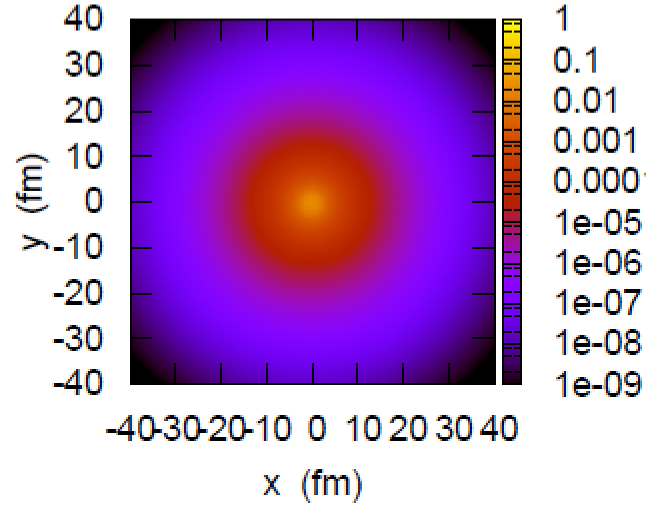

e = -0.21 MeV

V_0 = 10 MeV
R = 2.496 fm

Other candidates for 1n halo nuclei

^{19}C: S_n = 0.58(9) MeV

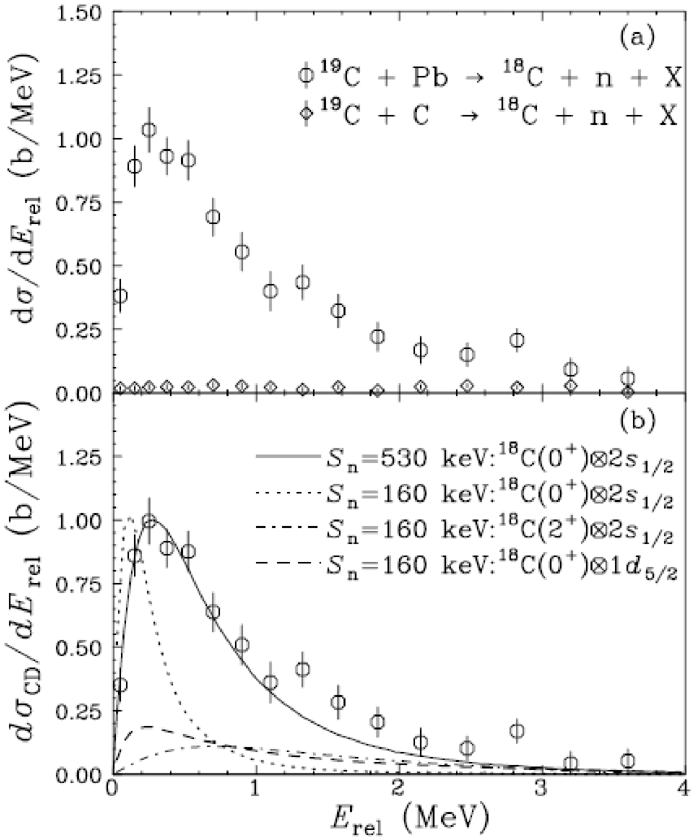

Coulomb breakup of ^{19}C

T. Nakamura et al., PRL83(‘99)1112

^{31}Ne: S_n = 0.29 +/- 1.64 MeV

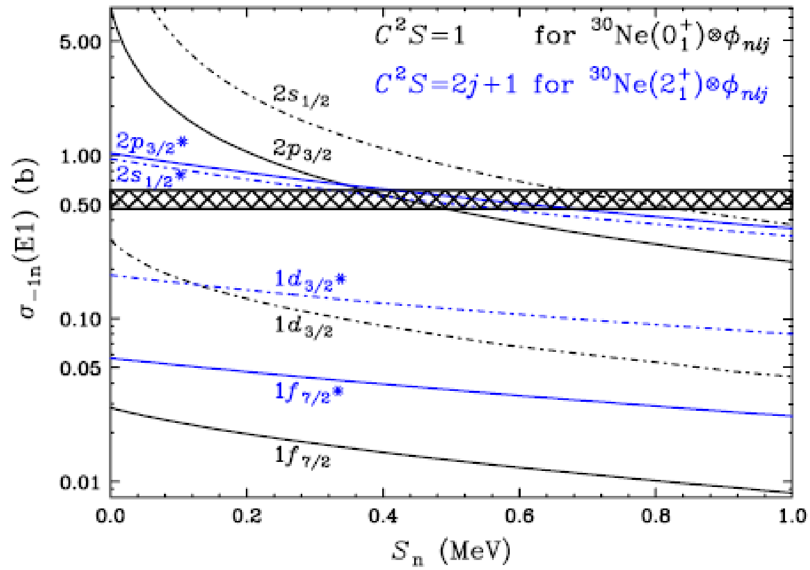

Large Coulomb breakup cross sections

T. Nakamura et al., PRL103(‘09)262501

Coulomb breakup of 1n halo nuclei

$^{A}Z \rightarrow {}^{A}Z^{*} \rightarrow {}^{A-1}Z + n$

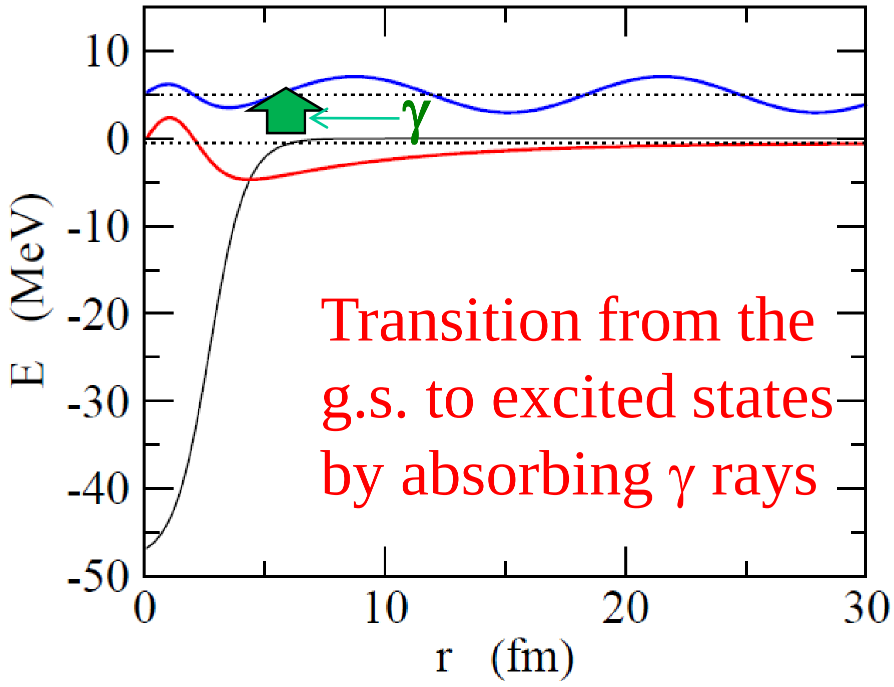

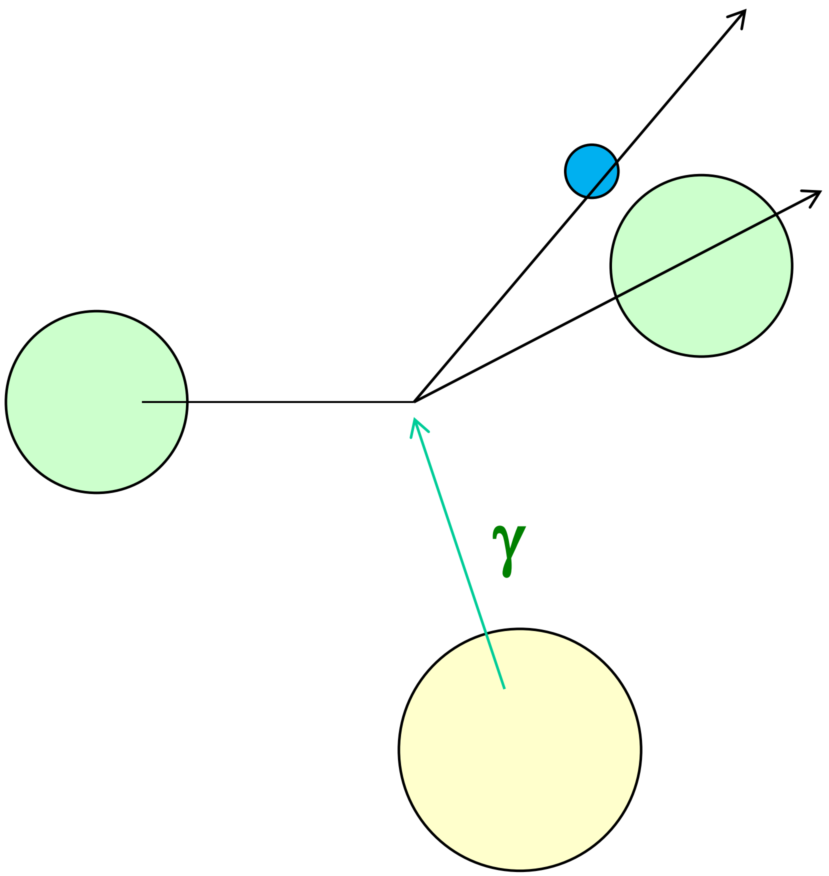

breakup if excited to continuum states ← excitations due to the Coulomb field from the target nucleus

Electromagnetic transitions

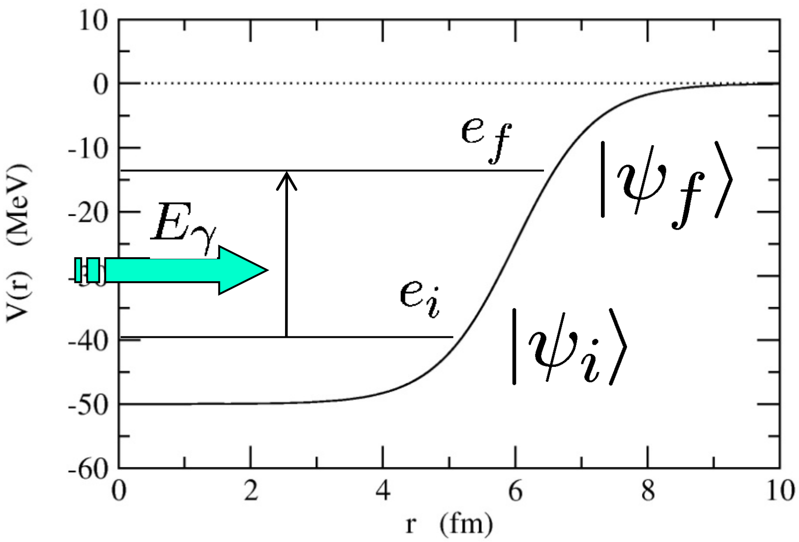

photon

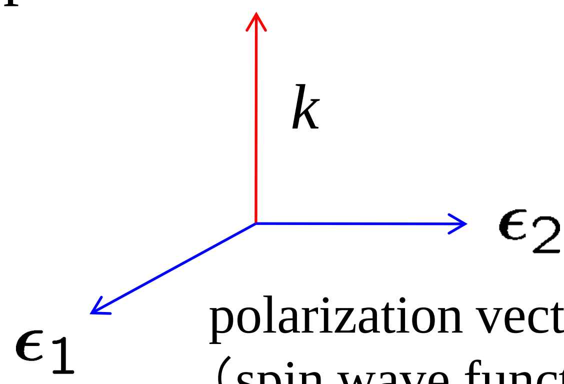

polarization vector
(spin wave function of photon)

initial state: $|\psi_i\rangle |n_{k\alpha} = 1\rangle$ ← State of nucleus: Ψ_i, + one photon with momentum k, and polarization α (α = 1 or 2)

transition ↓ H_{int} (interaction between a nucleus and EM field)

final state: $|\psi_f\rangle |n_{k\alpha} = 0\rangle$

Application to the present problem (in the dipole approximation):

$$\Gamma_{i\to f} = \frac{1}{2\pi\hbar}\left(\frac{Ze}{A+1}\right)^2 (e_f - e_i)\left|\langle\psi_f|z|\psi_i\rangle\right|^2 \delta(e_f - e_i - \hbar\omega)$$

$$P_{i\to f} \sim \left|\langle\psi_f|z|\psi_i\rangle\right|^2$$

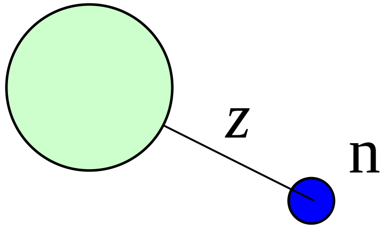

$$\sum_f P_{i\to f} =$$

Application to the present problem (in the dipole approximation):

$$\Gamma_{i\to f} = \frac{1}{2\pi\hbar}\left(\frac{Ze}{A+1}\right)^2 (e_f - e_i)\left|\langle\psi_f|z|\psi_i\rangle\right|^2 \delta(e_f - e_i - \hbar\omega)$$

$$P_{i\to f} \sim \left|\langle\psi_f|z|\psi_i\rangle\right|^2$$

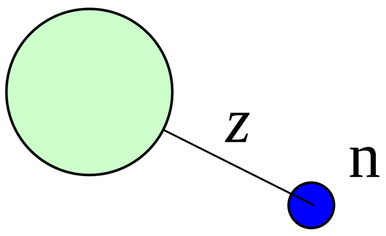

$$\sum_f P_{i\to f} = \sum_f \langle\psi_i|z|\psi_f\rangle\langle\psi_f|z|\psi_i\rangle$$
$$= \langle\psi_i|z^2|\psi_i\rangle$$

large transition probability if the spatial extention in *z* is large

Simple estimate of E1 strength distribution (analytic model)

Transition from an $l = 0$ to an $l = 1$ states:

WF for the initial state: $\Psi_i(\boldsymbol{r}) = \sqrt{2\kappa}\,\dfrac{e^{-\kappa r}}{r} Y_{00}(\hat{\boldsymbol{r}})$ $\kappa = \sqrt{\dfrac{2\mu|E_b|}{\hbar^2}}$

WF for the final state: $\Psi_f(\boldsymbol{r}) = \sqrt{\dfrac{2\mu k}{\pi\hbar^2}}\, j_1(kr) Y_{1m}(\hat{\boldsymbol{r}})$ $j_1(kr)$: spherical Bessel function

$k = \sqrt{\dfrac{2\mu E_c}{\hbar^2}}$

$$\frac{dB(E1)}{dE} = \frac{3}{4\pi} e_{E1}^2 \left| \int_0^\infty r^2 dr\, r \cdot \frac{\sqrt{2\kappa} e^{-\kappa r}}{r} \cdot \sqrt{\frac{2\mu k}{\pi\hbar^2}}\, j_1(kr) \right|^2$$

The integral can be performed analytically

$$\frac{dB(E1)}{dE} = \frac{3\hbar^2}{\pi^2\mu} e_{E1}^2 \frac{\sqrt{|E_b|}\, E_c^{3/2}}{(|E_b| + E_c)^4}$$

Refs. (for more general l_i and l_f)

- M.A. Nagarajan, S.M. Lenzi, A. Vitturi, Eur. Phys. J. A24('05)63
- S. Typel and G. Baur, NPA759('05)247

Wigner-Eckart theorem and reduced transition probability

$$\left|\langle\psi_f|rY_{10}|\psi_i\rangle\right|^2 \;\to\; \frac{1}{2l+1}\sum_{m,m'}|\langle\psi_{l'm'}|rY_{10}|\psi_{lm}\rangle|^2$$

$$= \frac{1}{3}\cdot\frac{1}{2l+1}\,|\langle\psi_{l'}||rY_1||\psi_l\rangle|^2$$

Reduced transition probability

$$\frac{dB(E1)}{dE_\gamma} = \frac{1}{2l+1}\left|\langle\psi_f||e_{\mathrm{E1}}rY_1||\psi_i\rangle\right|^2\delta(e_f - e_i - E_\gamma)$$

$$\frac{dB(E1)}{dE} = \frac{3\hbar^2}{\pi^2\mu} e_{E1}^2 \frac{\sqrt{|E_b|}\, E_c^{3/2}}{(|E_b| + E_c)^4}$$

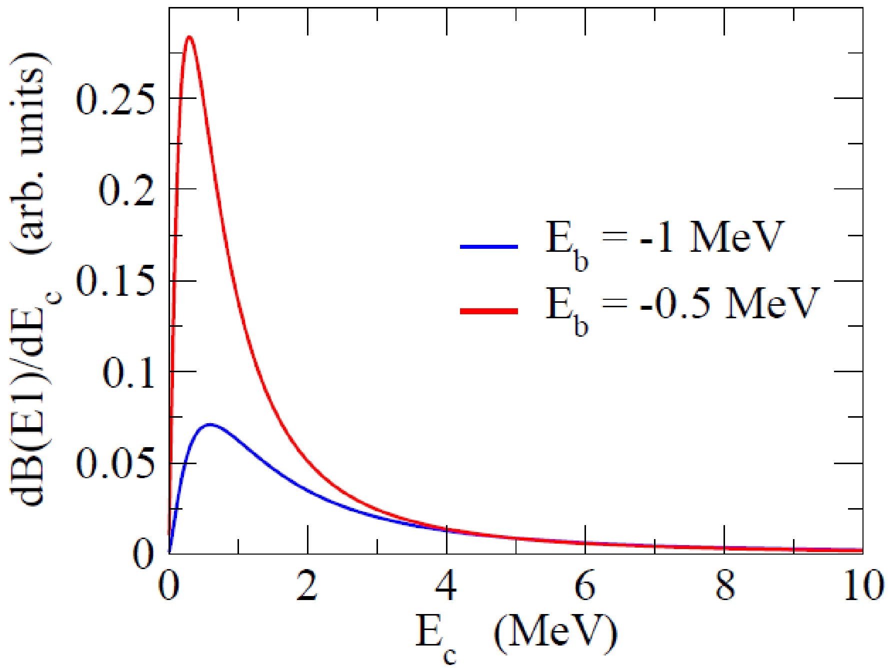

peak position: $E_c = \frac{3}{5}|E_b|$

$\left(E_x = E_c - E_b = \frac{8}{5}|E_b|\right)$

peak height: $\propto 1/|E_b|^2$

Total transition probability:

$$B(E1) = S_0 = \frac{3\hbar^2 e_{E1}^2}{16\pi^2\mu|E_b|}$$

- a high and sharp peak as the bound state energy, $|E_b|$, becomes small
- As the bound state energy, $|E_b|$, gets small, the peak appears at a low energy

E_{peak} = 0.28 MeV (E_b=-0.5 MeV)

cf. $\frac{3}{5}|E_b| = 0.3$ MeV

Sum Rule

$$S_0 = \int_0^\infty dE_c \frac{dB(E1)}{dE_c} = \frac{3}{4\pi} e_{E1}^2 \langle r^2 \rangle_i$$

Total E1 transition probability: proportional to the g.s. expectation value of r^2

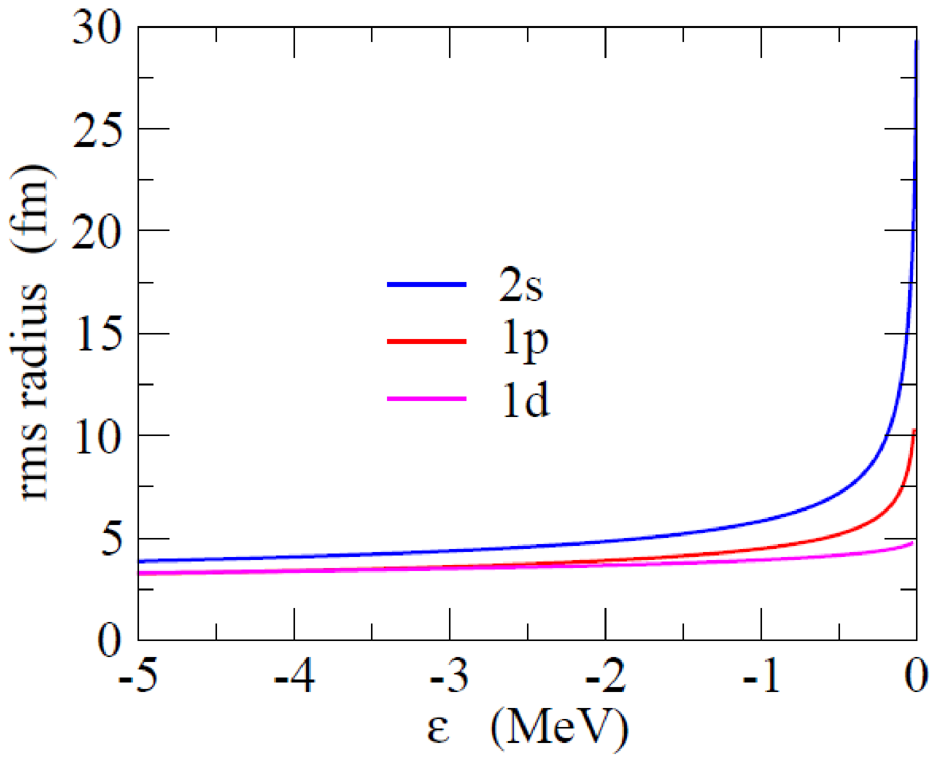

If the initial state is l=0 or l=1, the radius increases forweakly bound

Enhancement of total E1 prob.

Inversely, if a large E1 prob. (or a large Coul. b.u. cross sections) are observed, this indicates l=0 or l=1 ⟶ halo structure

Other candidates for 1n halo nuclei

^{19}C: S_n = 0.58(9) MeV

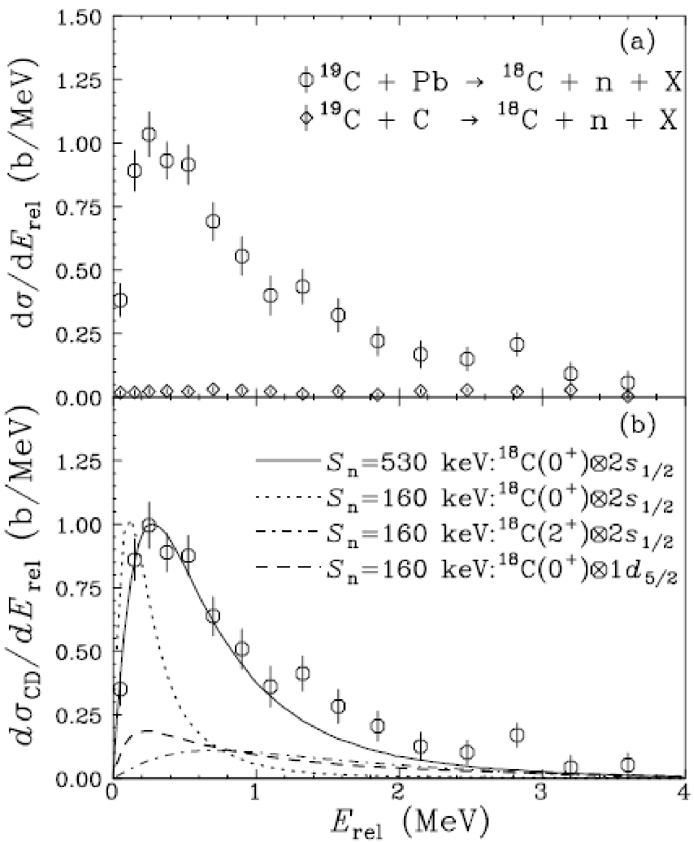

Coulomb breakup of ^{19}C

T. Nakamura et al., PRL83(‘99)1112

^{31}Ne: S_n = 0.29 +/- 1.64 MeV

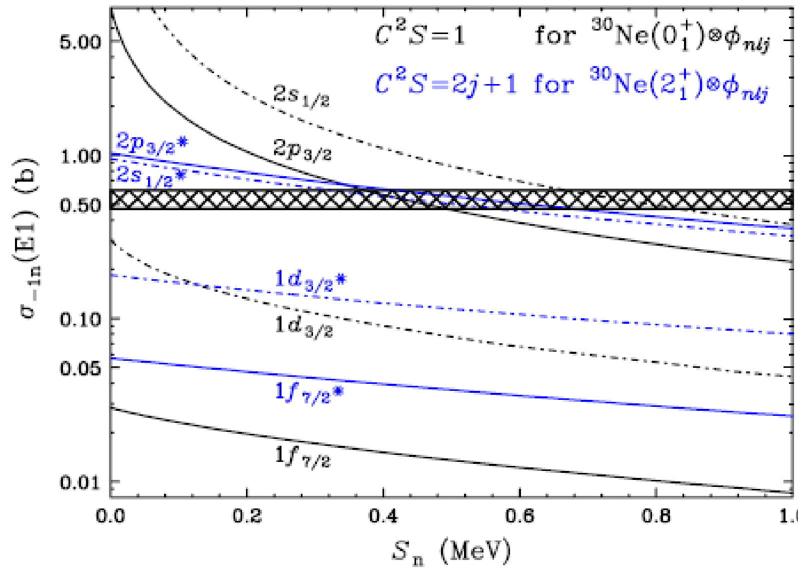

Large Coulomb breakup cross sections

T. Nakamura et al., PRL103(‘09)262501

Deformed halo nucleus

^{31}Ne

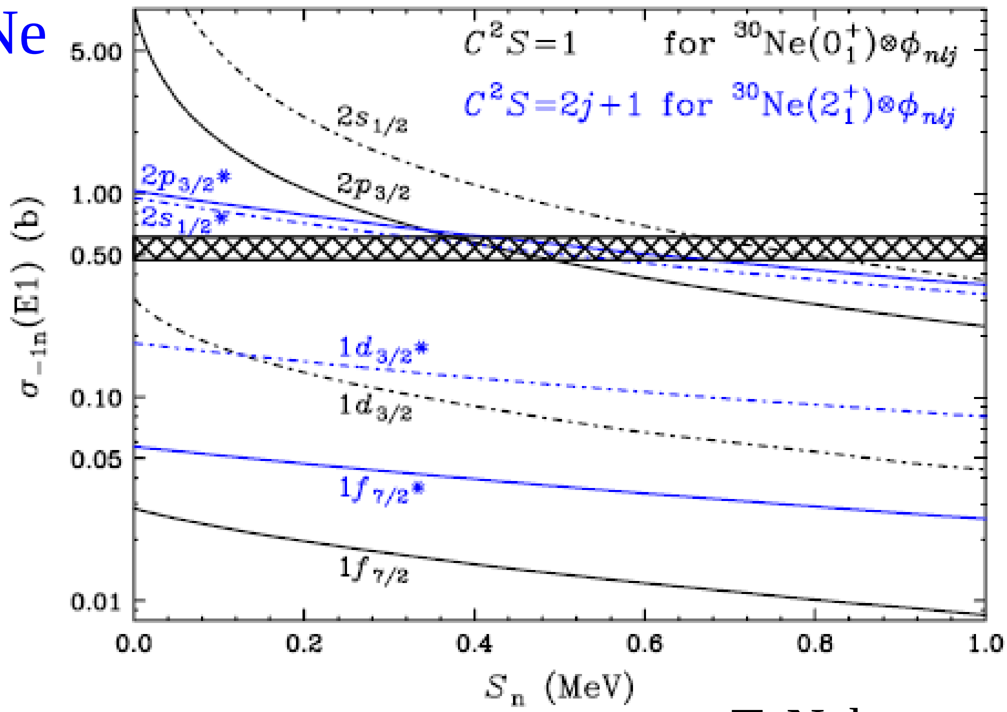

T. Nakamura et al.,
PRL103(‘09)262501

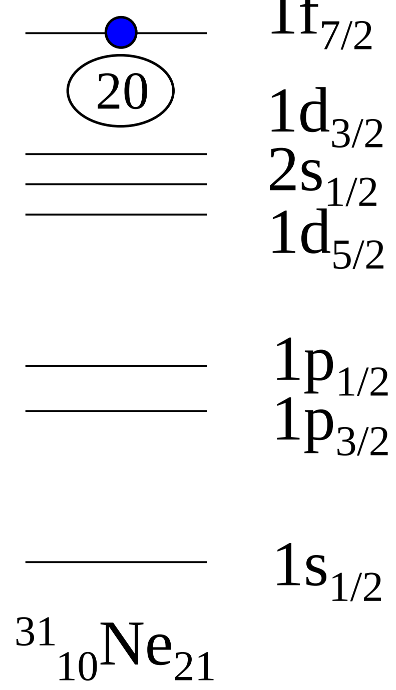

large Coulomb break-up cross sections

⟶ halo structure?

spherical potential
→ no halo (f-wave)

⟶ deformation?

Nilsson model analysis [I. Hamamoto, PRC81('10)021304(R)]

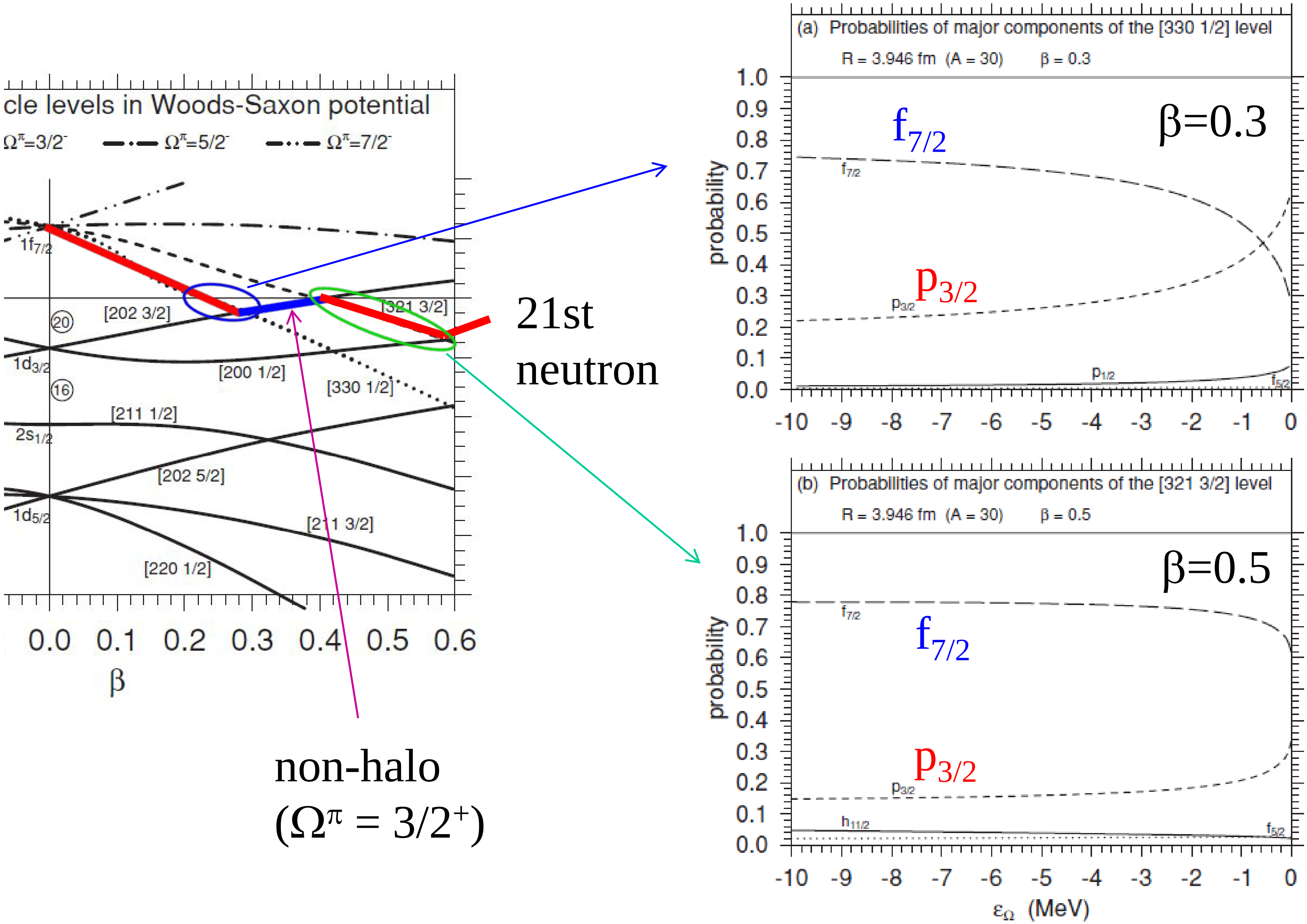

^{31}Ne

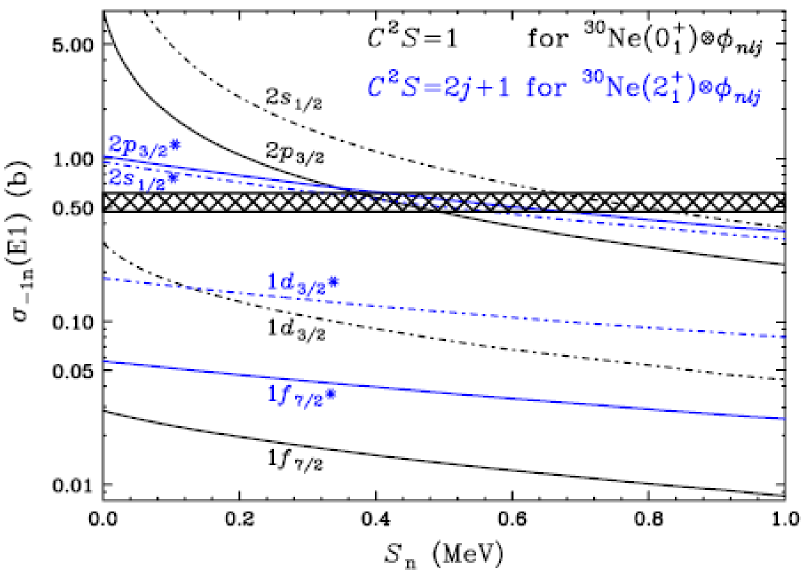

T. Nakamura et al.,
PRL103('09)262501

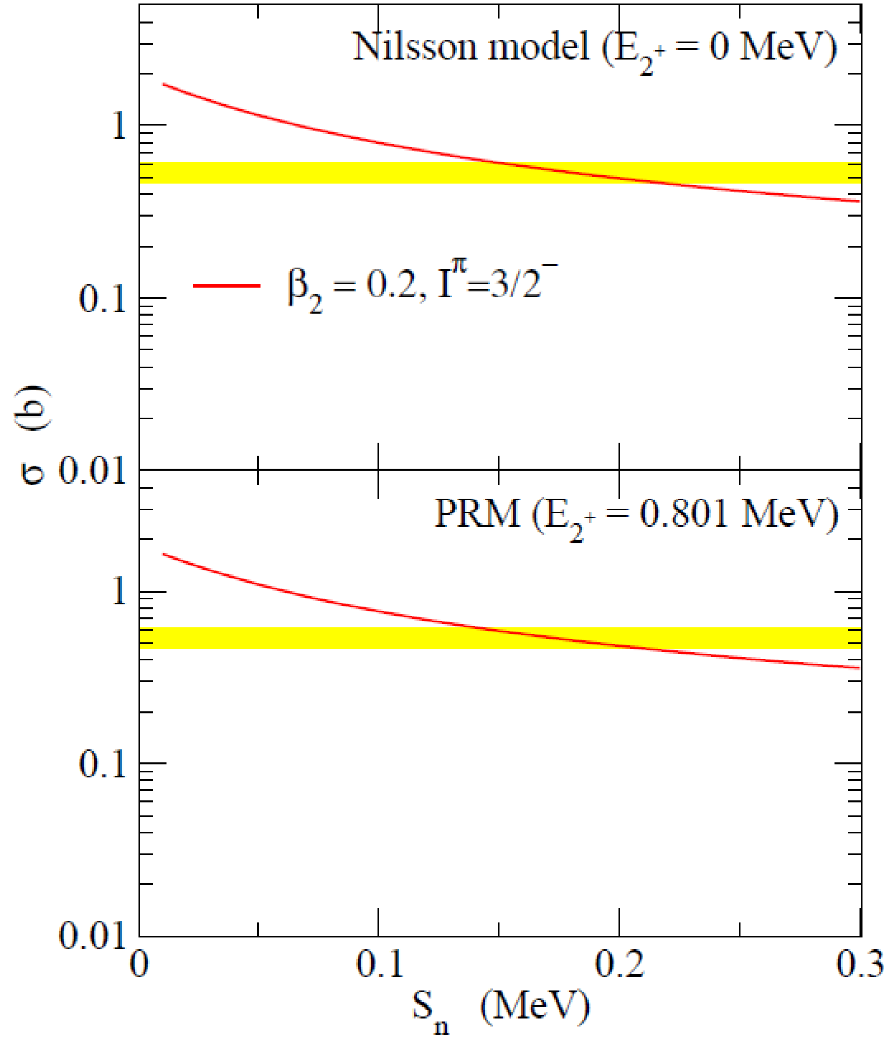

large Coulomb break-up
cross sections

E_{2+} (^{30}Ne) = 0.801(7) MeV
P. Doornenbal et al.,
PRL103('09)032501

S_n (^{31}Ne) = 0.29 +/- 1.64 MeV

Y. Urata, K.H., and H. Sagawa,
PRC83('11)041303(R)

2n halo nucleus

Three-body model : microscopic understanding of di-neutron correlation

^{11}Li, ^{6}He

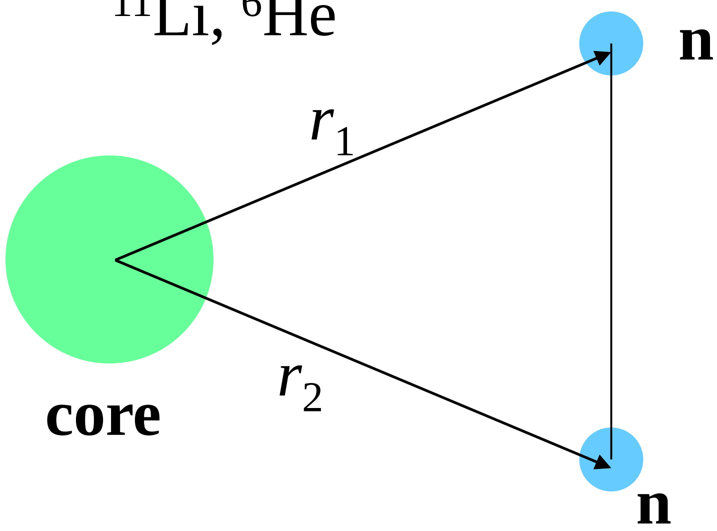

$$H = \frac{\boldsymbol{p}_1^2}{2m} + \frac{\boldsymbol{p}_2^2}{2m} + V_{nC}(r_1) + V_{nC}(r_2) + V_{nn}(\boldsymbol{r}_1, \boldsymbol{r}_2) + \frac{(\boldsymbol{p}_1 + \boldsymbol{p}_2)^2}{2A_c m}$$

(the last term: the recoil kinetic energy of the core nucleus in the three-body rest frame)

⇨ Obtain the ground state of this three-body Hamiltonian and investigate the density distribution

(e.g.,) expand the wf with the eigen-functions for H without V_{nn} and determine the expansion coefficients

$$\Psi_{gs}(\boldsymbol{r}_1, \boldsymbol{r}_2) = \mathcal{A} \sum_{nn'lj} \alpha_{nn'lj} \Psi^{(2)}_{nn'lj}(\boldsymbol{r}_1, \boldsymbol{r}_2)$$

$$\Psi^{(2)}_{nn'lj}(\boldsymbol{r}_1, \boldsymbol{r}_2) = \sum_m \langle jmj-m|00\rangle \psi_{nljm}(\boldsymbol{r}_1)\psi_{n'lj-m}(\boldsymbol{r}_2)$$

Comparison between with and without paring correlations

^{11}Li a distribution of one of the neutrons when the other neutron is at (z_1, x_1)=(3.4 fm, 0)

Without pairing $[1p_{1/2}]^2$

With pairing

- When no pairing, symmetric between *z* and –*z*.
  The distribution does not change whereever the 2nd neutron is.
- When with pairing, the nearside density is enhanced.
  The distribution changes when the 2nd neutron moves.

What is Di-neutron correlation?

Correlation: $\langle AB \rangle \neq \langle A \rangle \langle B \rangle$

Example: $^{18}O = {}^{16}O + n + n$

cf. $^{16}O + n$: 3 bound states ($1d_{5/2}$, $2s_{1/2}$, $1d_{3/2}$)

i) Without nn interaction: $|nn\rangle = |(1d_{5/2})^2\rangle$

Distribution of the 2nd neutron when the 1st neutron is at z_1 :

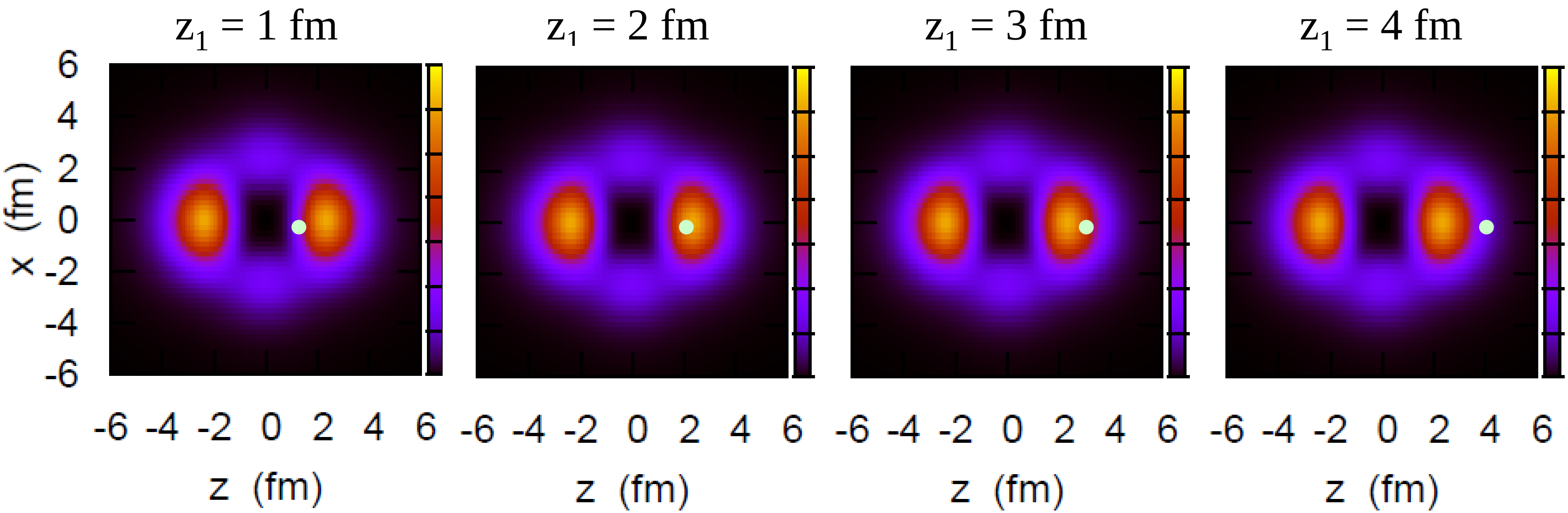

✓Two neutrons move independently

✓No influence of the 2nd neutron from the 1st neutron

$$\langle AB \rangle = \langle A \rangle \langle B \rangle$$

What is Di-neutron correlation?

Correlation : $\langle AB \rangle \neq \langle A \rangle \langle B \rangle$

Example: $^{18}O = {}^{16}O + n + n$

cf. ^{16}O + n : 3 bound states ($1d_{5/2}$, $2s_{1/2}$, $1d_{3/2}$)

ii) nn interaction: works only on the positive parity (bound) states

$$|nn\rangle = \alpha|(1d_{5/2})^2\rangle + \beta|(2s_{1/2})^2\rangle + \gamma|(1d_{3/2})^2\rangle$$

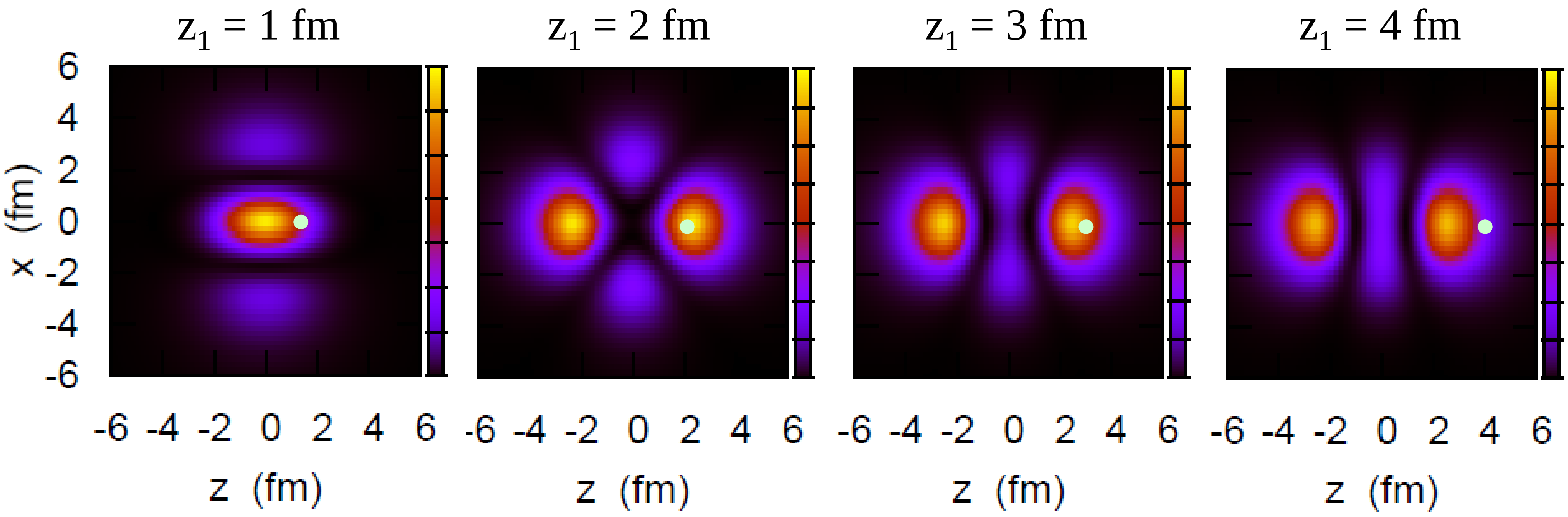

✓distribution changes according to the 1st neutron (nn correlation)

✓but, the distribution of the 2nd neutron has peaks both at z_1 and $-z_1$

⟶ this is NOT called the di-neutron correlation

What is Di-neutron correlation?

Correlation : $\langle AB \rangle \neq \langle A \rangle \langle B \rangle$

Example: ^{18}O = ^{16}O + n + n

cf. ^{16}O + n : 3 bound states ($1d_{5/2}$, $2s_{1/2}$, $1d_{3/2}$)

ii) nn interaction: works only on the positive parity (bound) states

$$|nn\rangle = \alpha|(1d_{5/2})^2\rangle + \beta|(2s_{1/2})^2\rangle + \gamma|(1d_{3/2})^2\rangle$$

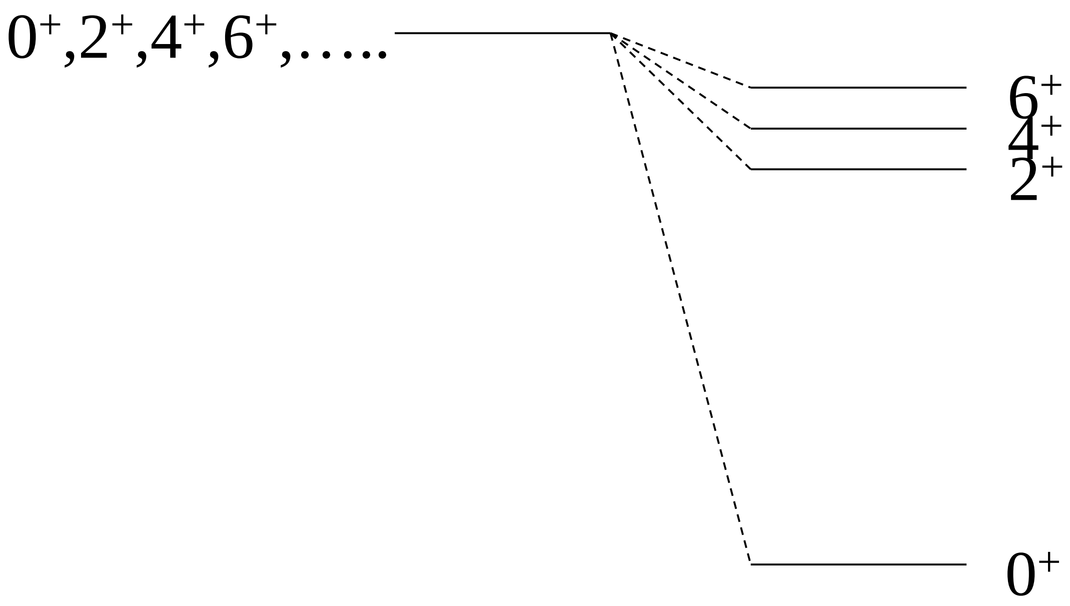

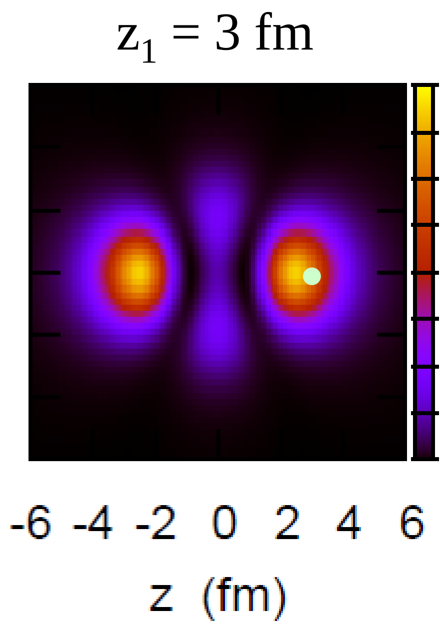

pairing correlation does not necessarily lead to a compact configuration (when the model space is stricted)

What is Di-neutron correlation?

Correlation : $\langle AB\rangle \neq \langle A\rangle\langle B\rangle$

Example: ^{18}O = ^{16}O + n + n

cf. ^{16}O + n : 3 bound states ($1d_{5/2}$, $2s_{1/2}$, $1d_{3/2}$)

iii) nn interaction: works also on the continuum states

$$|nn\rangle = \sum_{n,n',j,l} C_{nn'jl}|(nn'jl)^2\rangle$$

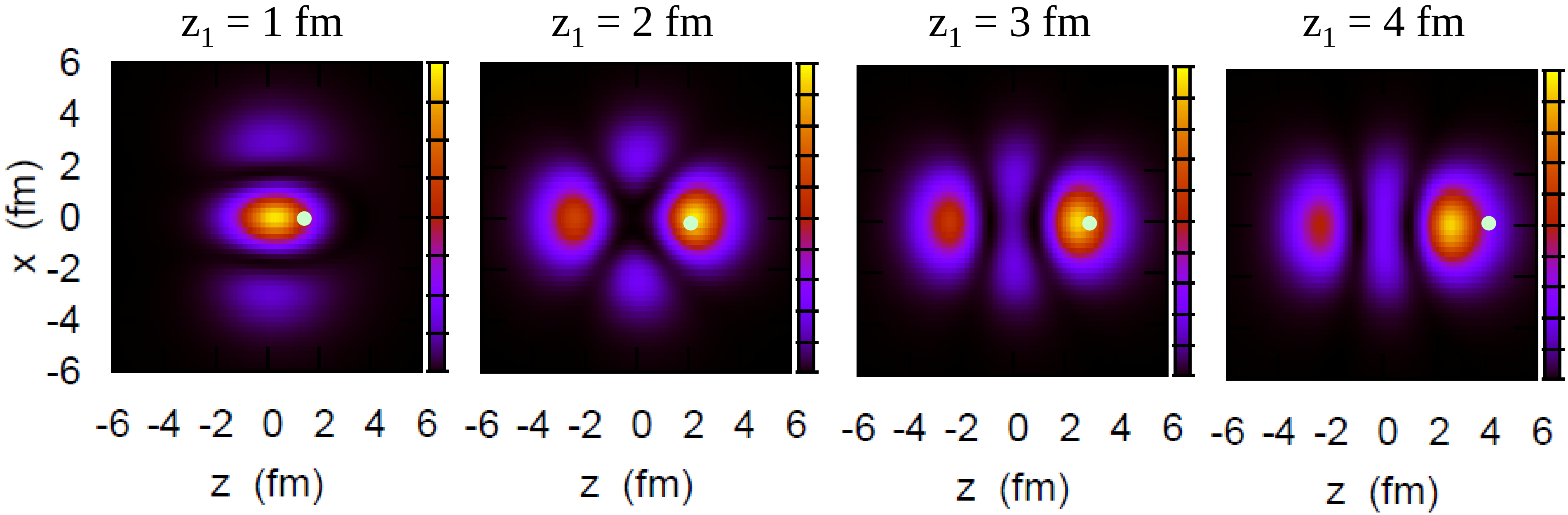

✓spatial correlation: the density of the 2nd neutron localized close to the 1st neutron (dineutron correlation)

✓parity mixing: essential role

cf. F. Catara et al., PRC29('84)1091

Example: $^{18}O = ^{16}O + n + n$ cf. $^{16}O + n$: 3 b.s. ($1d_{5/2}$, $2s_{1/2}$, $1d_{3/2}$)

i) positive parity only → insufficient

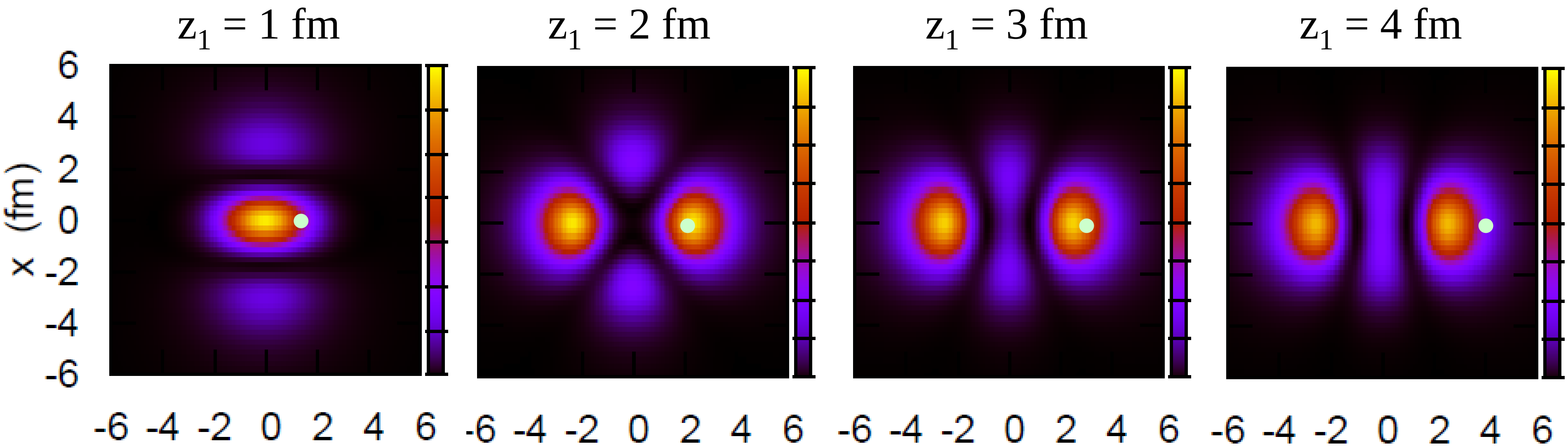

ii) **positive + negative parities (bound + continuum states)**

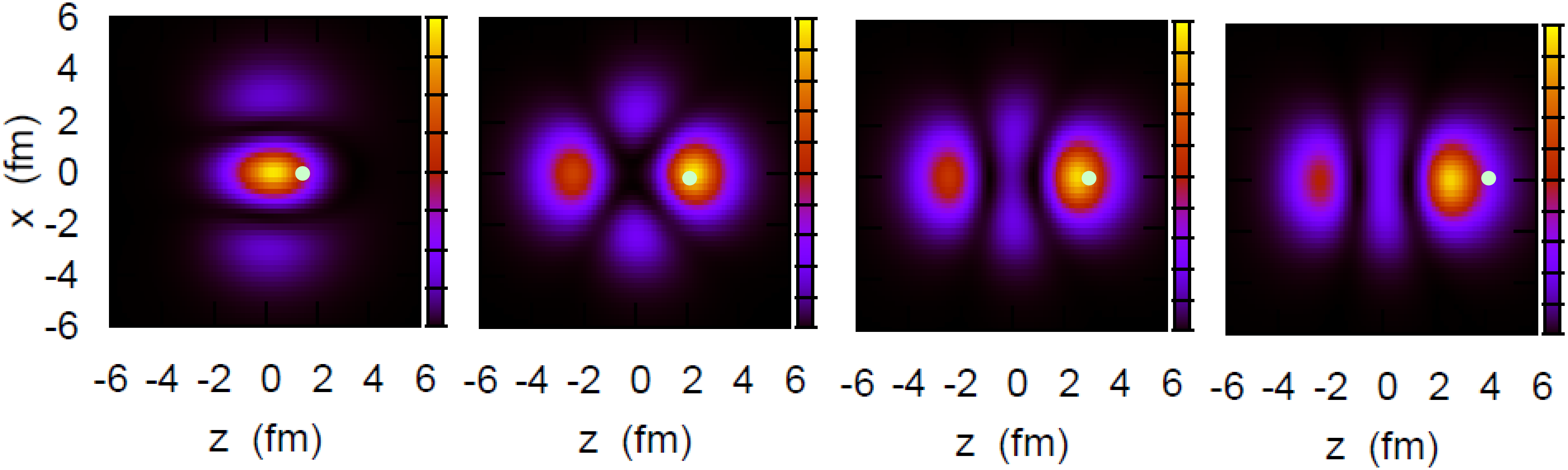

Recent topic: two-neutron decay of unbound ^{26}O nucleus

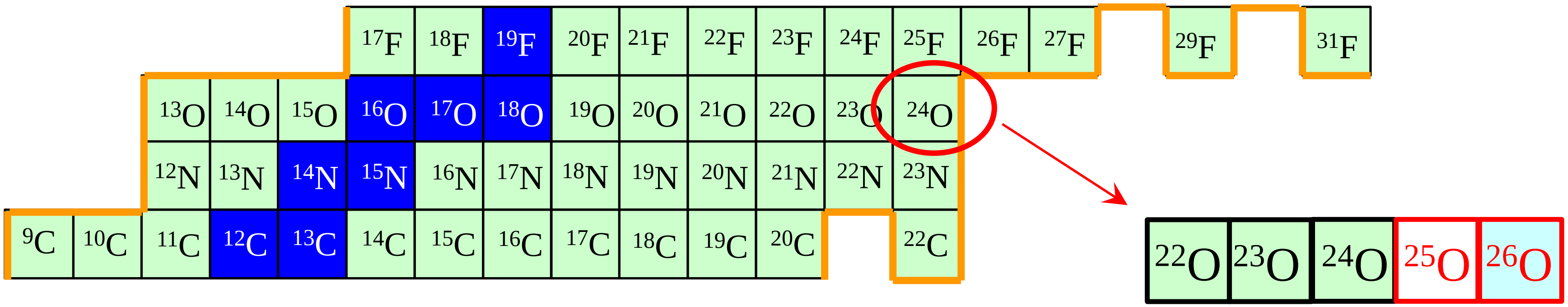

$$^{26}O \longrightarrow {}^{24}O + n + n$$

Expt. : $^{27}F \rightarrow {}^{26}O \rightarrow {}^{24}O + n + n$

- MSU: E. Lunderberg et al., PRL108 (‘12) 142503
- GSI: C. Caesar et al., PRC88 (‘13) 034313
- RIKEN: Y. Kondo et al., PRL116(’16)102503

Experimental data for decay spectrum

Expt. : $^{27}F \rightarrow {}^{26}O \rightarrow {}^{24}O + n + n$

- MSU: E. Lunderberg et al., PRL108 ('12) 142503
- GSI: C. Caesar et al., PRC88 ('13) 034313
- RIKEN: Y. Kondo et al., PRL116('16)102503

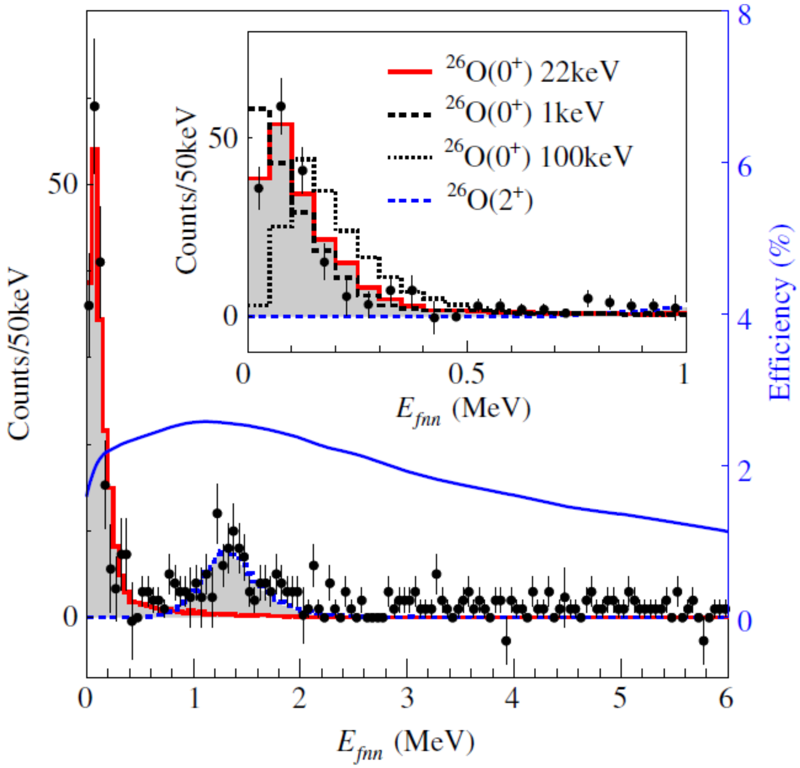

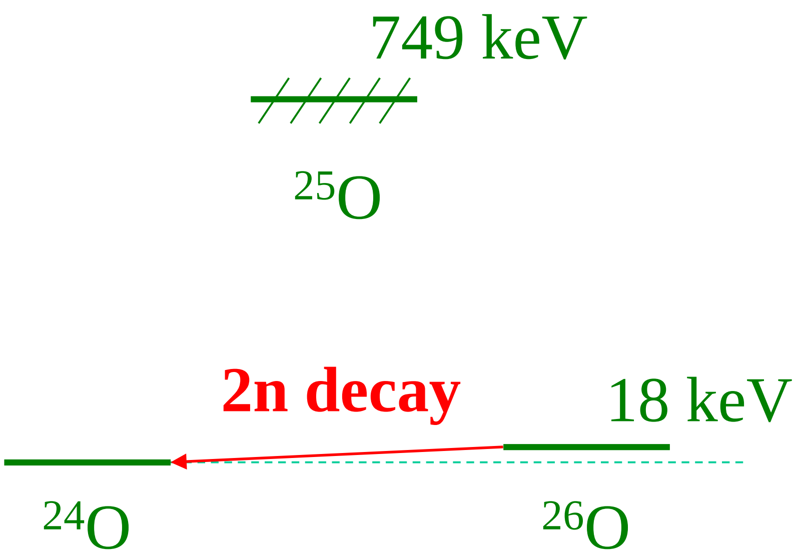

Y. Kondo et al., PRL116('16)102503 $\longrightarrow$ $E_{\text{decay}}(^{26}\text{O}) = 18 \pm 3 \pm 4$ keV

Decay energy spectrum

K.H. and H. Sagawa,
- PRC89 (‘14) 014331
- PRC93(‘16)034330

three-body model calculations

with nn interaction

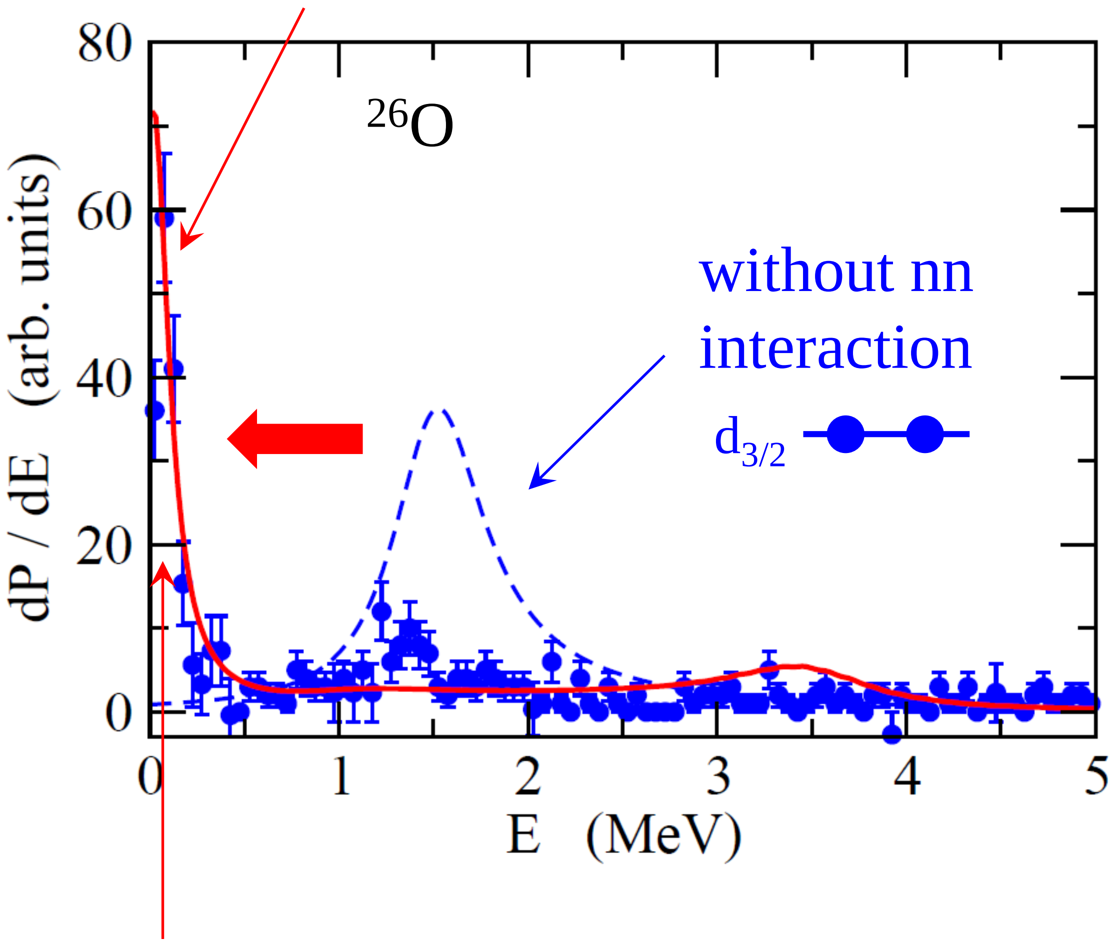

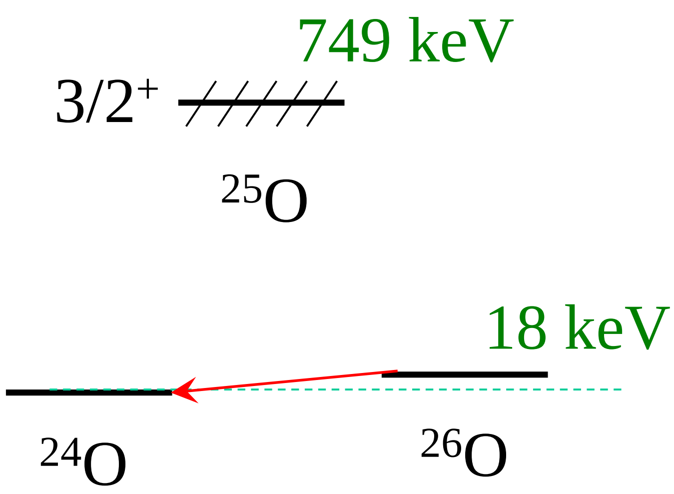

Data: Y. Kondo et al., PRL116(’16)102503

E_{peak} = 18 keV

Decay energy spectrum

K.H. and H. Sagawa,
- PRC89 ('14) 014331
- PRC93('16)034330

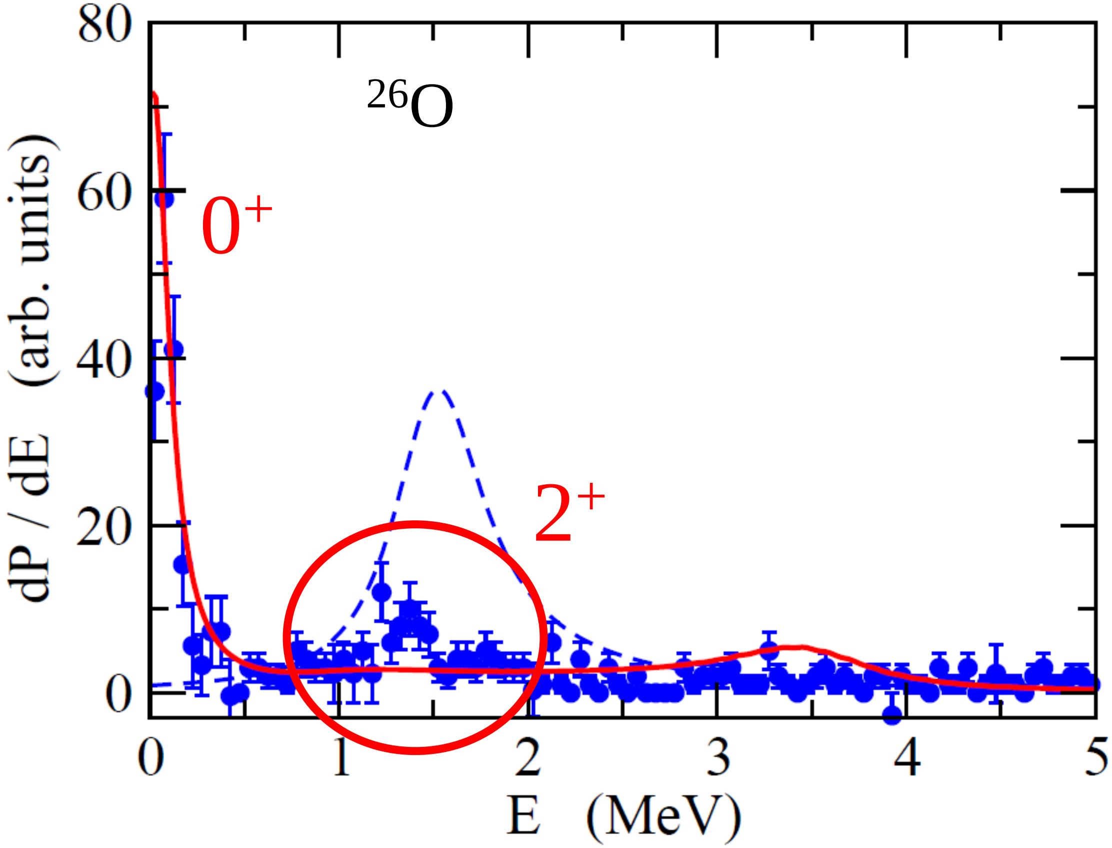

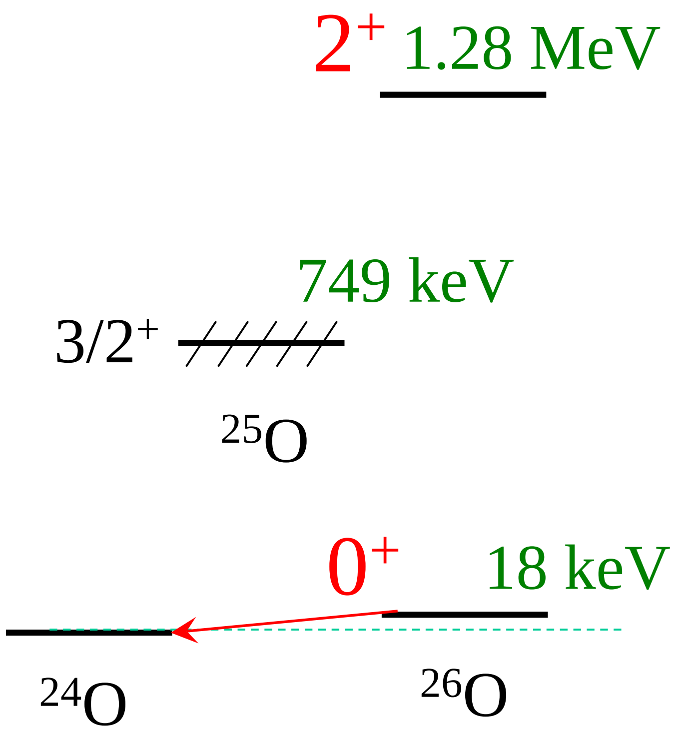

a prominent second peak
at $E = 1.28\,^{+0.11}_{-0.08}$ MeV

Data: Y. Kondo et al., PRL116('16)102503

a textbook example of pairing interaction!

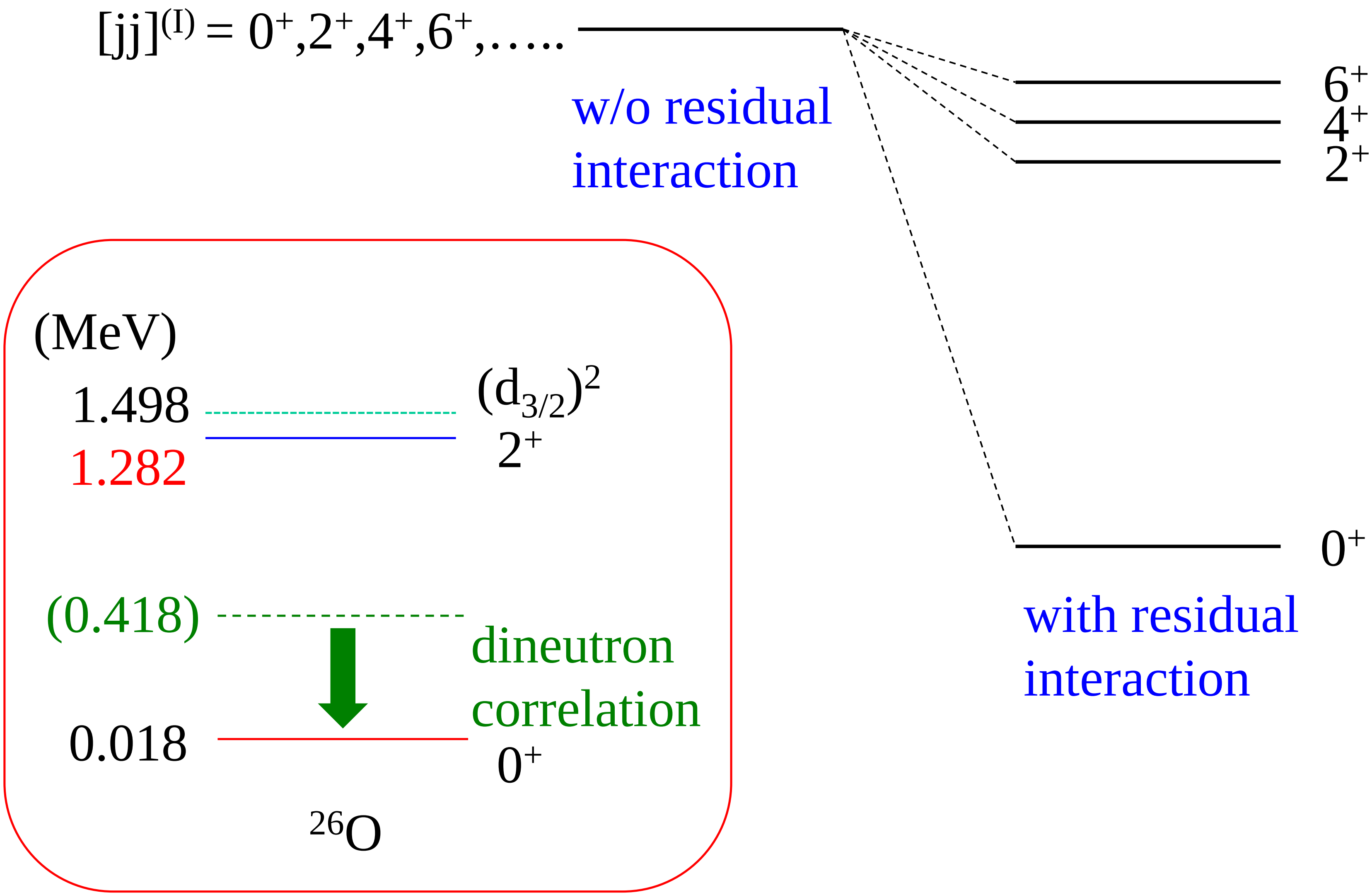

Decay of unbound nuclei beyond the drip lines

….as a probe for di-neutron correlations inside nuclei

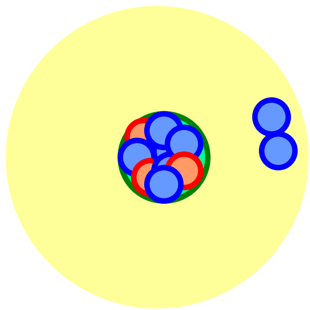

How to probe it?

- Coulomb breakup
  - ✓ disturbance due to E1 field
- two-proton decays
- two-neutron decays

spontaneous emission without a disturbance

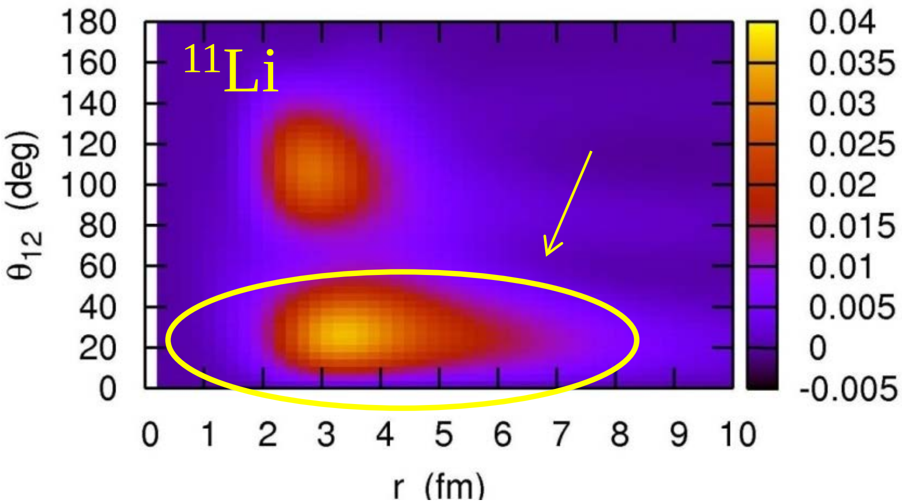

K.H. and H. Sagawa, PRC72 ('05) 044321

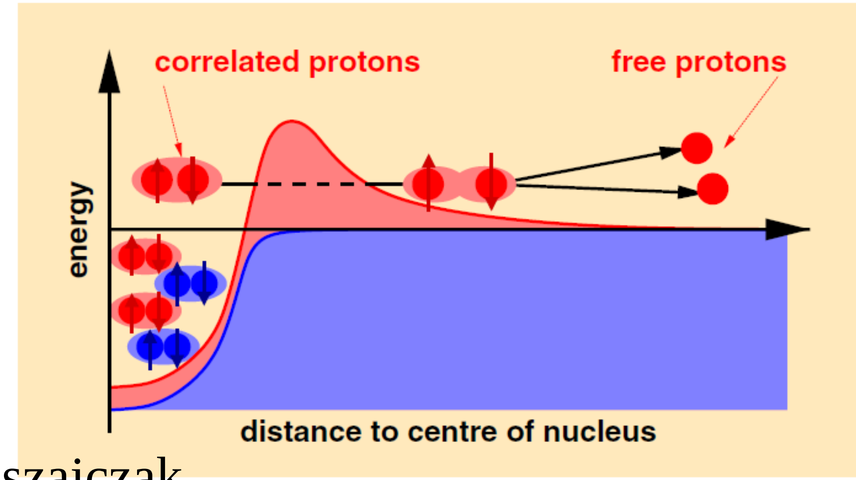

B. Blank and M. Ploszajczak,
Rep. Prog. Phys. 71('08)046301